Original article
https://doi.org/10.36233/0372-9311-161

Metabolome and exposome profiling of the biospecimens from COVID-19 patients in India

Shalini Aggarwal[1]*, Shashwati Parihari[1]*, Arghya Banerjee[1]*, Jyotirmoy Roy[2]*, Nirjhar Banerjee[1], Renuka Bankar[1], Saravanan Kumar[3], Manisha Choudhury[1], Rhythm Shah[4], Kharanshu Bhojak[4], Viswanthram Palanivel[1], Akanksha Salkar[1], Sachee Agrawal[5], Om Shrivastav[5], Jayanthi Shastri[5], Sanjeeva Srivastava[1]✉

[1]Department of Biosciences and Bioengineering, Indian Institute of Technology Bombay, Mumbai, India;
[2]Department of Chemical Engineering, Indian Institute of Technology Bombay, Mumbai, India;
[3]Thermo Fisher Scientific India | First Technology Place, Whitefield, Bangalore, India;
[4]Department of Metallurgical Engineering and Material Science, Indian Institute of Technology Bombay, Powai, Mumbai, India;
[5]Kasturba Hospital for Infectious Diseases, Chinchpokli, Mumbai, India

Abstract

Introduction. COVID-19 has become a global impediment by bringing everything to a halt starting from January 2020. India underwent the lockdown starting from 22nd March 2020 with the sudden spike in the number of COVID-19 patients in major cities and states. This study focused on how metabolites play a crucial role in SARS-CoV-2 prognosis.

Materials and methods. Metabolome profiling of 106 plasma samples and 24 swab samples from symptomatic patients in the Indian population of the Mumbai region was done. COVID-19 positive samples were further segregated under the non-severe COVID-19 and severe COVID-19 patient cohort for both plasma and swab.

Results. After analyzing the raw files, total 7,949 and 12,871 metabolites in plasma and swab were found. 11 and 35 significantly altered metabolites were found in COVID-19 positive compared to COVID-19 negative plasma and swab samples, respectively. Also, 9 and 23 significantly altered metabolites were found in severe COVID-19 positive to non-severe COVID-19 positive plasma and swab samples, respectively. The majorly affected pathways in COVID-19 patients were found to be the amino acid metabolism pathway, sphingosine metabolism pathway, and bile salt metabolism pathway.

Conclusion. This study facilitates identification of potential metabolite-based biomarker candidates for rapid diagnosis and prognosis for clinical applications.

Keywords: *plasma, swab, COVID-19, SARS-CoV-2, prognosis, biomarker candidate, metabolome, exposome, therapeutic target*

Ethics approval. The study was conducted with the informed consent of the patients. The research protocol was approved by the Institute Ethics Committee, Indian Institute of Technology Bombay, and Institutional Review Board, Kasturba Hospital for Infectious Diseases (approval code IITB-IEC/2020/030).

Acknowledgments. The authors would like to acknowledge the active support from Prof. Ambarish Kunwar from the Department of Biosciences & Bioengineering to fabricate UV transport device for sample transport and Prof. Anirban Banerjee for the BSL-2 biosafety aspects is gratefully acknowledged. MASSFIIT (Mass Spectrometry Facility, IIT Bombay) from the Department of Biotechnology (BT/PR13114/INF/22/206/2015) is gratefully acknowledged for MS-based proteomics work. The authors also acknowledge the "Thermo Fisher Scientific" engineers and application scientists for their support to our MASSFIIT facility during the extreme lock-down time.
All the figures were created using Servier Medical Art templates, licensed under a Creative Commons Attribution 3.0 Unported License.

Funding source. The study was supported through Science and Engineering Research Board, Department of Science & Technology, Ministry of Science and Technology, Government of India (SB/S1/Covid-2/2020), and a special COVID-19 seed grant (RD/0520-IRCCHC0-006) from IRCC, IIT Bombay to SS. The reported study was partially funded by RFBR according to the research project № 19-04-00088. The IIT Bombay fellowship supported Sh. Aggarwal and Sh. Parihari by the UAY-MHRD fellowship. Sh. Parihari was supported by CSIR. N. Banerjee is supported by DBT-JRF. A. Banerjee is supported by a CSIR fellowship, India.

Conflict of interest. The authors declare no apparent or potential conflicts of interest related to the publication of this article.

For citation: Aggarwal Sh., Parihari Sh., Banerjee A., Roy J., Banerjee N., Bankar R., Kumar S., Choudhury M., Shah R., Bhojak Kh., Palanivel V., Salkar A., Agrawal S., Shrivastav O., Shastri J., Srivastava S. Metabolome and exposome profiling of the biospecimens from COVID-19 patients in India. *Journal of microbiology, epidemiology and immunobiology = Zhurnal mikrobiologii, èpidemiologii i immunobiologii.* 2021;98(4):397–415.
DOI: https://doi.org/10.36233/0372-9311-161

* Authors are first Authors under equal contribution.

Original article
https://doi.org/10.36233/0372-9311-161

Метаболомное и экспосомное профилирование клинических образцов от пациентов с COVID-19 в Индии

Shalini Aggarwal[1]*, Shashwati Parihari[1]*, Arghya Banerjee[1]*, Jyotirmoy Roy[2]*, Nirjhar Banerjee[1], Renuka Bankar[1], Saravanan Kumar[3], Manisha Choudhury[1], Rhythm Shah[4], Kharanshu Bhojak[4], Viswanthram Palanivel[1], Akanksha Salkar[1], Sachee Agrawal[5], Om Shrivastav[5], Jayanthi Shastri[5], Sanjeeva Srivastava[1]✉

[1]Department of Biosciences and Bioengineering, Indian Institute of Technology Bombay, Mumbai, India;
[2]Department of Chemical Engineering, Indian Institute of Technology Bombay, Mumbai, India;
[3]Thermo Fisher Scientific India | First Technology Place, Whitefield, Bangalore, India;
[4]Department of Metallurgical Engineering and Material Science, Indian Institute of Technology Bombay, Powai, Mumbai, India;
[5]Kasturba Hospital for Infectious Diseases, Chinchpokli, Mumbai, India

Аннотация

Введение. COVID-19 стал глобальной проблемой начиная с января 2020 г. В Индии локдаун был введен 22 марта 2020 г. вследствие резкого роста числа пациентов с COVID-19 в крупных городах и штатах страны. Данное исследование посвящено изучению роли метаболитов в прогнозе исхода инфекции, вызываемой SARS-CoV-2.

Материалы и методы. Выполнено метаболомное профилирование 106 образцов плазмы и 24 образцов мазков от индийских пациентов с клиническими проявлениями инфекции, проживавших в регионе Мумбаи. Образцы плазмы и мазков пациентов с положительным результатом на COVID-19 были дополнительно разделены на две группы в соответствии с нетяжёлым и тяжёлым течением COVID-19.

Результаты. В результате анализа первичных данных были обнаружены 7949 и 12 871 метаболитов в образцах плазмы и мазков соответственно. По сравнению с COVID-19-отрицательными образцами в образцах плазмы и мазков от пациентов с COVID-19 были обнаружены 11 и 35 значительно изменённых метаболитов соответственно. Кроме того, в образцах плазмы и мазков от пациентов с тяжёлым COVID-19 выявлены 9 и 23 метаболита соответственно, значительно изменённые по сравнению с образцами от пациентов с нетяжёлым течением COVID-19. Обнаружено, что COVID-19 оказывает наибольшее влияние на метаболические пути, связанные с метаболизмом аминокислот, сфингозина и солей желчных кислот.

Заключение. Результаты данного исследования способствуют идентификации потенциальных кандидатов в биомаркёры на основе метаболитов для быстрой диагностики и прогноза в клинической практике.

Ключевые слова: *плазма, мазок, COVID-19, SARS-CoV-2, прогноз, кандидатные биомаркеры, метаболом, экспосом, терапевтическая мишень.*

Этическое утверждение. Исследование проводилось при добровольном информированном согласии пациентов. Протокол исследования одобрен Этическими комитетами Indian Institute of Technology Bombay и Institutional Review Board, Kasturba Hospital for Infectious Diseases (код утверждения IITB-IEC/2020/030).

Благодарность. Авторы хотели бы выразить признательность профессору Ambarish Kunwar из Департамента биологических наук и биоинженерии за активную поддержку в изготовлении УФ-транспортного устройства для транспортировки образцов и профессору Anirban Banerjee за обеспечение биобезопасности уровня BSL-2. MASSFIIT (Mass Spectrometry Facility, IIT Bombay) из Департамента биотехнологии (BT/PR13114/INF/22/206/2015) проводили исследования по протеомике на основе MS. Авторы также выражают признательность инженерам и специалистам «Thermo Fisher Scientific» за их поддержку предприятия MASSFIIT во время экстремальной ситуации локдауна.
Все рисунки были созданы с использованием шаблонов Servier Medical Art под лицензией Creative Commons Attribution 3.0.

Источник финансирования. Исследование было поддержано Советом по научным и инженерным исследованиям Департамента науки и технологий Министерства науки и технологий правительства Индии (SB/S1/Covid-2/2020), а также специальным грантом по изучению COVID-19 (RD/0520-IRCCHC0-006) от IRCC, IIT Bombay для SS. Настоящее исследование частично финансировалось RFBR в соответствии с исследовательским проектом № 19-04-00088. Sh. Aggarwal и Sh. Parihari являются стипендиатами UAY-MHRD от IIT Bombay. Sh. Parihari был поддержан CSIR, N. Banerjee — DBT-JRF, A. Banerjee — стипендией CSIR, Индия.

Конфликт интересов. Авторы декларируют отсутствие явных и потенциальных конфликтов интересов, связанных с публикацией настоящей статьи.

Для цитирования: Aggarwal Sh., Parihari Sh., Banerjee A., Roy J., Baneerjee N., Bankar R., Kumar S., Choudhury M., Shah R., Bhojak Kh., Palanivel V., Salkar A., Agrawal S., Shrivastav O., Shastri J., Srivastava S. Метаболомное и экспосомное профилирование клинических образцов от пациентов с COVID-19 в Индии. *Журнал микробиологии, эпидемиологии и иммунобиологии.* 2021;98(4):397–415.
DOI: https://doi.org/10.36233/0372-9311-161

* Авторы являются первыми авторами с равным вкладом.

Introduction

The SARS-CoV-2 virus in COVID-19 imitates febrile and respiratory diseases in humans such as influenza in various ways, including clinical symptoms, host immune response to viral infection, and virus transmission in the host body [1]. Clinical symptoms in these two respiratory diseases are quite similar which include mainly fever, chills, headache, muscle pain, tiredness, sore throat, stuffy nose, difficulty in breathing, and acute respiratory distress syndrome (ARDS) etc. [2, 3]. However, SARS-CoV-2 infection also results in dry coughs, anosmia or ageusia, aphonia, chest pain, skin rashes rarely, discoloration of fingers and toes, and organ failure [1, 3]. Organ failure has also been observed in risk-free, healthy individuals in case of long COVID-19 [4]. In COVID-19 cases, ARDS mostly affects patients with co-morbidities such as diabetes mellitus, hypertension, cancer, and kidney diseases [5, 6]. The diagnostic tests available for influenza are more robust, including rapid influenza diagnostic tests (RIDTs), RT-PCR molecular assays, and antibody-based immunofluorescent assays, whereas rapid diagnostic tests with high specificity and sensitivity in COVID-19 are awaited [1, 7].

Metabolites are another aspect using which one can diagnose or differentiate the diseased condition from a healthy one. Metabolites are easy to extract from the different sample sources and have been studied vastly for various diseases and disorders such as cancer [8], Lyme disease [9], tuberculosis [10], and pediatric autism spectrum disorders [11]. Metabolites are small biomolecules with less than 1,000 Da, which play a crucial role in managing pathways in any organism [12]. Metabolites meticulously act at all the stages of the central dogma and regulates various pathways [13, 14]. Therefore, a metabolomics study will help us better understand the mechanisms involved in the pathology of SARS-CoV-2. This can help in finding the potential targets for vaccination, drug exploration, or repurposing of FDA-approved drugs. There are various FDA-approved drugs available for the treatment of influenza respiratory disease, including amantadines, oseltamivir, laninamivir, and others [15]. However, there are no specified FDA-approved drugs available for COVID-19 treatment. However, due to the paucity of time and pandemic sequelae due to the virulent nature of the pathogen, scientists have looked into the repurposing of broad spectrum antibiotics, FDA-approved antibiotics such as hydroxychloroquine, azithromycin, and remdesiver [16–18]. Few animals based and *in vitro* studies have shown the positive effect of chloroquine against SARS-CoV [19–21] and avian influenza [22]. Hence, antimalarial FDA-approved drugs may have a synergistic effect with macrolides such as azithromycin in ablation of the viral pathology but lacks strong evidence *in vivo* system [23].

Furthermore, various chemicals and biomolecules from the environment have been reported to affect the disease progression in synergy with genetic makeup and microbial load. Although human health is significantly dependent upon environmental exposures, the diversity and variation in exposures are poorly understood [24]. The visible gap in understanding the chemical-specific disease risks and human metabolic pathways indicates that a more global approach towards systems biology [25] is the need of the hour to expand beyond the endogenous metabolome to the exposome [26]. Exposomics reveals the exogenous chemicals an individual gets exposed to during his lifetime. As blood acts as the medium of transport for chemicals to and from the tissues, it also represents a reservoir of all endogenous and exogenous chemicals at a given time [27, 28]. Several reports have shown that the transmission of the SARS-CoV-2 virus and the disease progression in each individual depends on the infection characteristics such as viral load, prevalent co-morbidities, and the host of exposures belonging to the exogenous or endogenous human exposome domains [29, 30].

Therefore, in this study, along with a comprehensive metabolomics analysis of individual plasma and nasopharyngeal swab samples from COVID-19 patients with different severity of infection, we performed the blood exposome analysis. In the metabolomics study, we found the significantly altered and most frequently reported creatinine and indole-3-acetic acid in the COVID-19 severe sample cohort compared to COVID-19 non-severe sample cohort [31, 32]. Also, propionylcarnitine, monoglycerides and cis-stilbene oxide in the same plasma samples comparison but not frequently reported. We also found threo-sphingosine, phytosphingosine, myristamide, herniarin, butoctamide and 3-hydroxy-3-methylpentanedioic acid altered in swab samples of severe COVID-19 as compared to non-severe COVID-19 sample cohorts. We further carried out pathway analysis for understanding the role of significantly altered metabolites on various human biological pathways by using published data and our experimental data. The most consistent and recurring metabolites may form the basis for the future development of new prognostics and therapeutic intervention in a precise manner. In addition, we also report 3 significant blood exposomes (2-benzothiazolylthio) acetic acid, tabun, contrastigmin, deoxymethyl-SA, which correlate with the metabolic pathways to differentiate the COVID-19 positive cohort COVID-19(+) from negative cohort COVID-19(–).

The aim of the present study was to analyze the alteration in the metabolite levels using an untargeted metabolomics approach in swab and plasma samples from patients with COVID-19. This study will provide significant knowledge on the underlying disease mechanism and the significantly altered metabolites can be potential candidate biomarkers for disease prognosis and serve as therapeutic targets.

DOI: https://doi.org/10.36233/0372-9311-161

Materials and methods

Sample and clinical details

In this study, the leftover plasma and swab samples collected for routine hematological tests and COVID-19 RT-PCR tests were collected from Kasturba Hospital, Mumbai. All samples were collected with the approval from the Institute Ethics Committee, IIT Bombay and Institutional Review Board, Kasturba Hospital for infectious diseases. Informed consent was not required as leftover samples from the routine tests were processed for the study. Patients with confirmed COVID-19 status based on RT-PCR test results were included in the study.

The inclusion criteria include:

- RT-PCR report positive and negative;
- severe and non-severity decided on basis of WHO guidelines.

The exclusion criteria considered were:

- a female patient who is pregnant at enrolling;
- patient aged below 18.

As advised by the clinicians, COVID-19(+) patients were categorized into non-severe (patients with mild fatigue, fever, cough, and breathlessness with non-invasive ventilation) — NSC and severe (patients with bilateral pneumonia and acute respiratory distress symptoms with mechanical ventilation support) — SC [33]. In total, 106 plasma samples and 24 swab samples were processed for metabolome profiling. The study cohort included plasma samples from 31 patients with COVID-19(–) patients, 43 NSC patients, and 29 samples from SC patients. Similarly, swab samples from COVID-19(–) patients (n = 5), NSC (n = 9) and SC (n = 5) were included in the study. The age, gender distribution, hematological parameters, and biochemical parameters of the patients enrolled in the study can be found in **Table 1**.

Samples were viral inactivated using ethanol, processed and stored at –20°C until transportation of the samples to the IIT Bombay campus in cold storage was conducted in a month duration. The sample preparation protocols for plasma and swab were optimized at IIT Bombay by referring to the viral inactivation method used in B. Shen *et al.* [34]. All the steps were performed in the BSL level 3 facility at the hospital.

Sample preparation from plasma and swab samples

The plasma and swab samples were prepared using the same methodology as K. Suvarna *et al*. [35], overview of the workflow can be refered in **Fig. 1**.

Basic data analysis was done using "Compound Discoverer 3.0" software ("Thermo Fisher") with a threshold value of 100,000 for intensity marked as a signal. Experimental design, standard mix for instrument general quality check (QC), and internal standards for sample preparation QC were also set.

The internal standards were added at two different time points:

- while preparing samples to check sample preparation quality;
- while injecting samples in the mass spectrometer (MS) to check instrument functionality while running a particular sample.

After the sample run, during data analysis, the first step was to check the coefficient of variance in all the run sets, followed by CV among all the samples in a run and then PCA analysis of all QC pools run with each set. If the CV was less than 30% among the sets or individual sample runs, then the data was considered good to be taken forward (**Fig. 2**). Also, proper segregation of QC pools for all the sets represented the proper execution of the experiment (**Fig. 3**). This included the addition of various adduct ions naturally present in the plasma, which might alter the ion formation of the metabolite targets in question. Hence the most abundant adduct ions were selected for the exploration of the target metabolites.

Mass spectrometry of plasma and swab metabolites

The extracted samples containing internal standard were analyzed using Ultraperformance Liquid Chromatography–High-Resolution Mass Spectrometry (UPLC–HRMS) methods with positive ion mode of Electrospray Ionization (ESI). Each sample was run in triplicates, where one run was set for MS/MS analysis for identification of the metabolites. The rest two runs for each sample were used as technical replicates for acquiring MS data of extracted metabolites. The resolution of the mass spectrometer was set at 140,000 for full MS and 17,500 for ddMS2 and scanned at a mass range 100–700 m/z. The capillary, probe, autosampler and column temperatures were 340°C, 380°C, 4°C and 40°C, respectively. Sheath Gas flow rate at 42, Aux Gas rate at 10, and spray voltage at 3.8 kV. A C18 column, i.e., Hypersil GOLD (100 × 2.1 mm, 1.9 μm particle size, "Thermo Fisher Scientific", USA), was used in the UHPLC (Ultimate 3000) using water and 100% methanol as eluents both added with 0.1% formic acid, in a 20 mins gradient. The gradient consecutively reached 1% of methanol at 2 mins, 50% methanol at 5 mins, 98% methanol at 14 mins, stayed at 98% till 17 mins, 1% at 17.2 mins, and stayed at 1% methanol till 20 mins with a flow rate of 0.350 mL/min.

The samples were run in batches, and each sample was analyzed in three technical replicates using MS only and MS2 modes. Each batch of samples had initial blank runs consisting of 50% methanol, and a single blank was run after every sample. QC control samples consisting of a pool of samples were also run after every 5 samples to check the consistency of the instrument performance.

Statistical analysis

Analysis of acquired data was initially performed with the "Compound Discoverer 3.0" software ("Ther-

Table 1. Clinical information of the samples incorporated in the study

Parameter	Norm	Plasma samples			Swab samples		
		COVID-19(–)	NSC	SC	COVID-19(–)	NSC	SC
A. Patient information							
Number of participants		33	38	34	5[#]	11[##]	4
Age, years		50 (26–77)	52 (22–77)	56 (34–77)	43 (34–50)	53 (19–87)	55 (40–73)
B. Gender							
Males		20 (60.60)	23 (60.52)	20 (60.52)	2 (66.6)	7 (77.77)	2 (50)
Females		13 (39.39)	15 (39.47)	14 (39.47)	1 (33.3)	2 (22.22)	2 (50)
C. Patient status							
Discharged		30 (90.90)	35 (92.10)	19 (55.26)	3 (100)	9 (100)	2 (50)
Dead		0	2 (5.5)	15 (44.10)	0	0	2 (50)
Transfer/DAMA[ϕ]		3 (9.09)	1 (2.6)	0	0	0	0
Duration of hospital stay		50 (25–77)	10 (2–26)	23 (2–95)	4 (2–6)	7 (6–8)	18 (8–26)
Ventilation required		14 (30.43)	5 (13.18)	34 (100)	0	2 (2.22)	4 (100)
D. Hematological parameters							
Hemoglobin, g/dl		12.3 (8.7–16.6)	12 (5–14)	12 (7–15.4)	12.5 (10.4–15)	12.4 (9.4–15.7)	11.25 (10–13)
Polymorphs, %	40–75	71 (51–90)	68 (42–90)	78 (38–90)	65–87)	73 (57–90)	77 (58–85)
Lymphocytes, %	20–40	29 (10–49)	31 (10–58)	21 (10–62)	24 (13–35)	26 (10–43)	24 (15–42)
Platelets, lakhs/ul	1.5–4.5	1.82 (0.76–4)	2 (1–4)	2 (0.4–4.2)	1.13 (0.7–1.8)	1.9 (1.4–2.9)	2
E. Biochemical parameters							
SGOT, U/L	0–40	60 (30–176)*	68 (20–440)**	52 (25–87)	44 (33–53)	40 (24–75)	45 (36–53)
SGPT, U/L	5–34	33 (12–82)*	44 (11–250)**	36 (16–75)	34 (29–42)	20 (14–34)	22 (10–42)
AlkPO4, IU/L	15–112	80 (44–259)*	69 (34–102)**	70 (40–202)	40 (35–48)	65 (46–117)	57 (50–70)
Total bilirubin		0.8 (0.6–2)	1.9 (0.5–39.8)**	0.8 (0.6–1.4)	0.7 (0.7–0.8)	0.6 (0.6–0.8)	0.6 (0.6–0.8)
D. billirubin, mg%	0–0.3	0.2 (0.2–0.9)	0.7 (0.2–17.1)**	0.2 (0.2–1.10)	0.3 (0.3–1)	0.2	0.2
Total protein, gm%	6–8.4	6.93 (6.20–7.90)	7 (6–8.2)	6.39 (5.3–7.6)	0.2 (0.2)	6.9 (6.2–8.1)	6.6 (5.9–7)
Albumin, gm%	3.2–5.0	3.65 (3.00–4.20)	3.53 (2.5–4.5)	3.27 (2.6–4.5)	3.6 (3.2–4)	3.7 (3.3–4.6)	3.1 (2.4–3.9)
Globulin, gm%	2.0–2.5	3.27 (2.5–4.1)	3.3 (2.5–4.5)	3.17 (2.4–4.4)	2.7 (2.5–3)	3.2 (2.8–3.5)	3.5 (3–4)
Sodium, mEq/l	133–146	136 (129–143)	136 (124–142)	135 (120–151)	135 (131–138)	135 (132–142)	135 (129–142)
Potassium, mEq/l	3.8–5.6	4.16 (2.7–6.8)	4.1 (3.2–5.2)	4.31 (2.8–8.2)	4 (3.4–4.5)	7.4 (3.6–33.0)	3.65 (3.2–4)
Blood urea nitrogen, mg%	6–21	15 (5–100)	13.2 (5–34)	26.8 (1.9–220.0)	1.2 (1.1–1.5)	12 (6–29)	17 (10–25)
Creatinine, mg%	1–2	1.27 (0.6–6.4)	1.17 (0.80–2)	1.48 (0.7–10.0)	1.4 (0.9–2.9)	1.2 (0.8–2.0)	1.15 (1–1.4)
D-dimer, ng FEU/ml	<500	N/A	N/A	2765 (10–15000)	N/A	N/A	2221 (1972–2471)
C-reactive protein, mg/l	<5	N/A	N/A	26.97 (0.9–88.8)	N/A	N/A	7.85 (4.2–11.5)
Ferretin, ng/ml	22–322	N/A	N/A	1286.4 (99.3–12098.0)	N/A	N/A	385.7 (209.5–538.9)
Interleukin-6, pg/ml	0–7.0	N/A	N/A	84.3 (4.6–441.0)	N/A	N/A	7.88 (6.73–9.04)

Note. *In COVID-19(–) plasma samples, 3 patients show an unusual increase in the clinical parameters due to the co-morbidities. Patient 261 had thyroid and 262 had hypertension.
**Plasma sample of one COVID-19(+), NSC patient showed unusual increase in the LFT parameters as the patient had autoimmune hepatitis.
[#] No clinical data available for 2 patients from the COVID-19(–) group.
[##] No clinical data available for 2 samples.
[ϕ]DAMA – discharged against medical advice.

JOURNAL OF MICROBIOLOGY, EPIDEMIOLOGY AND IMMUNOBIOLOGY. 2021; 98(4)
DOI: https://doi.org/10.36233/0372-9311-161
ORIGINAL RESEARCHES

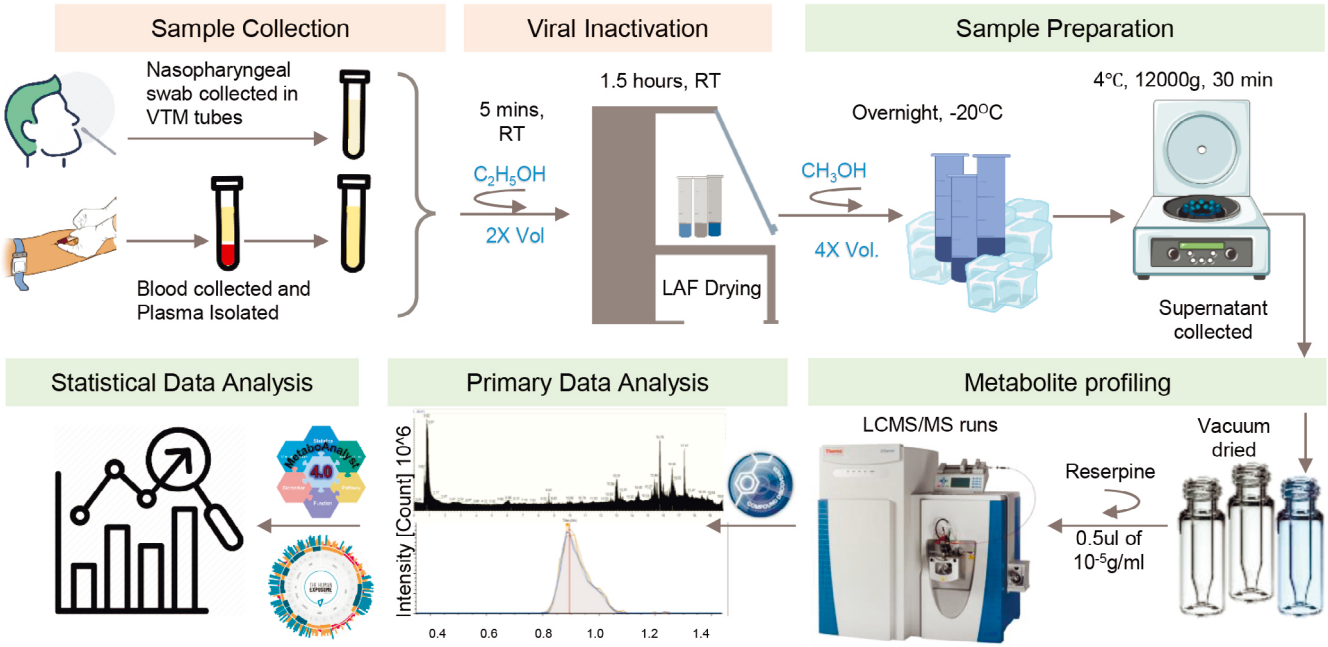

Fig. 1. Workflow of the metabolome profiling experiment using plasma and swab samples.

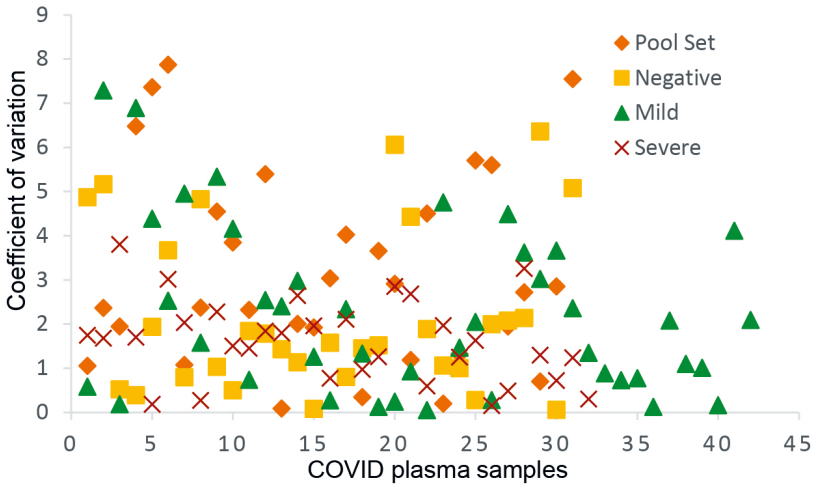

Fig. 2. Coefficient of variation of internal standard in COVID-19 plasma samples.

mo Fisher") for metabolite identification/quantitation, chromatography peak alignment, mass spectrum visualization, and statistical analysis. The workflow template used in "Compound Discoverer 3.0" includes unknown compound detection, peak alignment, predicting the compound's composition, and database searching against ChemSpider, which comprises of BioCyc, KEGG, and Human Metabolome Database (HMDB) with a mass tolerance of 5 ppm. For compound detection signal to noise ratio (S/N) was kept as 3, and the minimum peak intensity was 10^6. To assign compound annotation on MS/MS level, three different data sources, such as mzCloud, ChemSpider, and Metabolika, with a mass tolerance of 5 ppm, were used [36]. All the duplicate runs were treated as individual samples in the data analysis.

The "Compound Discoverer 3.0" analyzed output had three types of metabolite representation:

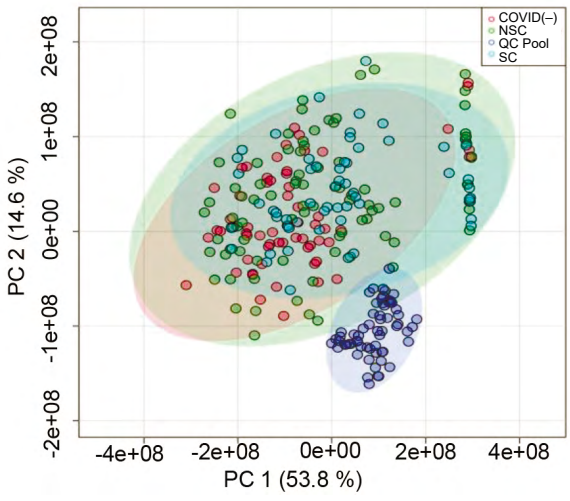

Fig. 3. PCA plot for all the plasma samples used in the study.

1. Metabolites with name, molecular formula, molecular mass, and retention time.

2. Metabolites without a name but with the molecular formula, molecular mass, and retention time.

3. Metabolites with molecular mass and retention time but no name and molecular formula.

No filtering was done at the beginning of the study to avoid loss of the data, and all the metabolites were given a code with the prefix "Meta_XX".

The QC pools and internal standards were checked in different batches (***Fig. S1**, A*[1]) to decide the normalization and transformation strategy. Spearman correlation analysis of each cohort and all the samples was performed to check the data quality, and the samples having R^2 above 0.5 were considered for further post-processing. Also, the CV of the internal standard was checked across the set of samples and individual samples. The samples passing CV% <30 for internal standards were only used in the data analysis. The features with over 30% missing values were filtered out, and the missing value imputation was done separately for each cohort through KNN (k-nearest neighboring) in "Metaboanalyst 4.0" [37, 38]. The data was then log-transformed and median normalized, which was followed by a two-tailed unpaired student *t*-test for each pair of cohorts. The compounds having FDR adjusted p-value less than 0.05 and $\log_2$ fold change above 1.5 were considered statistically differentially expressed metabolites. The experimental MS/MS spectra of the significant metabolites were compared to available reference MS/MS spectra in METLIN and HMDB for MSI level annotation.

The significant metabolites were also checked for their correlation within sample cohorts and were analyzed using "Cytoscape 3.8.2" with Java 11.0.6 application based on pathway mapping against KEGG pathway library for *Homo sapiens*.

Exposome analysis

The list of all the unannotated metabolites post CD analysis was taken for exposome exploration analysis. The analysis was done for all COVID-19 patients from the three categories: negative, NSC, and SC. The unannotated metabolites from the list was taken and mapped on the blood exposome database. The basis of mapping exposomes was the molecular formula, which was the common parameter between the raw files and the blood exposome database. The compounds with redundant chemical formulas were removed from the database to avoid ambiguity, which lead to loss of data. Once the exposomes were discovered for each cohort of patients, then comparative analysis was done for the groups: COVID-19(+) *vs.* COVID-19(–), and NSC *vs.* SC. Subsequently, T-test and fold change analysis was performed, and an exposome was considered statistically significant if it has *p*-value < 0.05 and fold change >1.5.

A detailed search was carried for all of the significantly altered exposomes to correlate them to various drugs, diseases and food habits. Relevant literatures were obtained from PubChem, PubMed, blood exposome database, US environmental protection agency website and DrugBank online. This information was correlated with the drugs and treatment administered to the patients to get an insight on how these compounds affect the biological pathways during the course of COVID-19.

Pathway analysis

The significant metabolites from both plasma and swab metabolite cohort were used to map the human metabolomics pathways. The list of the significant metabolites was subjected to "Metaboanalyst 4.0" under pathway analysis function. The metabolites mapped to HMDB IDs or KEGG IDs were segregated and the remaining unmapped metabolites were manually searched for their HMDB/KEGG ID. The final list of all the significant metabolites was again subjected to "Metaboanalyst 4.0" and pathways analysis using Fisher's exact test as enrichment method, scatter plot for visualization, relative betweenness centrality for topology mapping, and SMPDB pathway library.

Results

The workflow of metabolome profiling for plasma and swab samples is shown in Fig. 1. The QC control and internal standard for all the plasma samples are shown in Figs. 2, 3. The proper segregation of COVID-19(+) and COVID-19(–) plasma samples are shown in **Figs. 4–6**. The proper segregation of COVID-19 NSC and SC plasma samples is shown in **Figs. 7–9**. The PCA plot for representing proper segregation of QC pools from all swab sample run is shown in **Fig. 10**. The proper segregation of COVID-19(+) and COVID-19(–) swab samples is shown in **Fig. 11**. The proper segregation of COVID-19 NSC and SC swab samples is shown in **Figs. 12–14**.

Plasma metabolome of COVID-19 patient cohorts

On analysis of COVID-19(–) and COVID-19(+) samples, 11 metabolites were found to be common yet significantly differentially expressed metabolites (DEMs) after blank subtraction, having FDR adjusted *p*-value less than 0.05 and fold change above 1.5 (***Table S1***). Of the 11, 3 metabolites — l-α-glycerylphosphorylcholine, arachidonic acid and 1728235/monoacylglyceride — were found to be level-2 MSI (**Table 2**). The MS/MS spectra were matched with available online databases like MassBank of North America (MoNA) and HMDB. Dioctyltin, bis(4-ethylbenzylidene), sorbitol, 2210856, and 1728235 were level-3 MSI. Meta_2147, Meta_1992, and Meta_2701

[1] Supplemented materials see on the web page of the journal: http://www.jmei.ru

JOURNAL OF MICROBIOLOGY, EPIDEMIOLOGY AND IMMUNOBIOLOGY. 2021; 98(4)
DOI: https://doi.org/10.36233/0372-9311-161
ORIGINAL RESEARCHES

belong to level-4 MSI, whereas Meta_2208 and Meta_3308 were found to be level-5 MSI (*Table S1*).

The volcano plot shows 11 significantly altered metabolites in the COVID-19(+) and COVID-19(–) patient cohort; of these 5 metabolites are upregulated in the positive cohort and the rest 6 metabolites are downregulated (**Fig. 4**). These 11 metabolites were used to plot the PCA plot (**Fig. 5**) and heat map and showed the segregation of COVID-19(+) from COVID-19(–) (**Fig. 6**). The box plots represent annotated metabolites i.e., 6 out of 11 significant DEMs (Fig. 4), and boxplots for unannotated metabolites are represented in ***Fig. S1***, *B*).

A total of 24 significantly altered metabolites were found on comparing NSC with SC. Of the 24 significant metabolites, only 9 metabolites were found to be from samples and not contributed by blank. Propionylcarnitine, creatine, indole-3-acetic acid, glycochenode-

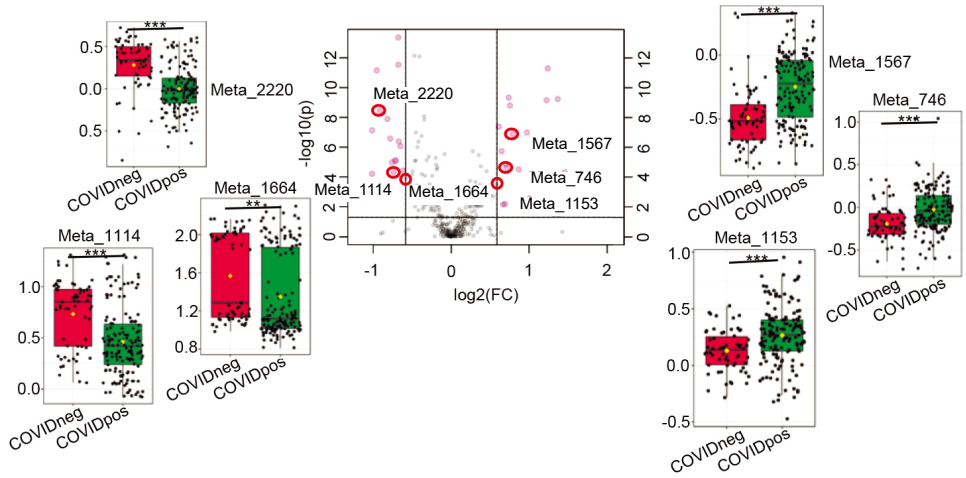

Fig. 4. Volcano plot representing the trend of significant metabolites in COVID-19(+) patients as compared to COVID-19(–) patients.

Table 2. List of significant metabolites from Plasma of COVID-19(–), mild and severe clinical cohorts

MSI level	Meta	Name	Pathways mapped to	Formula	RT	Log_2(FC)	FDR adjusted *p* value
List of differentially expressed metabolites in COVID-19(+) patients as compared to COVID-19(–) patients							
Level 2	Meta_746	l-Alpha-glycerylphosphorylcholine	Retinol metabolism	$C_8H_{20}NO_6P$	1.232	–0.72413	6.06E-05
Level 2	Meta_1153	Arachidonic acid	α-Linolenic acid and linoleic acid metabolism, arachidonic acid metabolism	$C_{20}H_{32}O_2$	20.047	–0.58732	0.000903
Level 2	Meta_1664	1728235/monoacylglyceride	–	$C_{19}H_{38}O_4$	19.949	0.59142	0.005183
Level 3	Meta_2220	Dioctyltin	–	$C_{16}H_{34}S$	20.361	0.91546	1.31E-08
Level 3	Meta_1114	Bis(4-ethylbenzylidene)sorbitol	–	$C_{24}H_{30}O_6$	13.395	0.74415	4.5E-06
Level 3	Meta_1567	2210856	–	$C_{18}H_{32}O_2$	20.131	–0.7918	3.39E-08
List of differentially expressed metabolites in NSC patients as compared to SC patients							
Level 2	Meta_222	Propionylcarnitine	Oxidation of branched chain fatty acids	$C_{10}H_{19}NO_4$	1.263	0.82397	0.0001733
Level 2	Meta_1023	Creatine	Glycine, serine and threonine metabolism, arginine and proline metabolism	$C_4H_9N_3O_2$	1.167	1.0631	2.1047E-05
Level 2	Meta_772	Indole-3-acetic acid	Tryptophan metabolism	$C_{10}H_9NO_2$	8.539	–1.0757	8.9473E-05
Level 2	Meta_1664	1728235/monoacylglyceride		$C_{19}H_{38}O_4$	19.949	–1.682	0.035002
Level 2	Meta_820	Glycochenodeoxycholic acid	Bile acid biosynthesis	$C_{26}H_{43}NO_5$	15.366	–1.7471	0.0052997
Level 2	Meta_1529	2-methylbutyrylcarnitine		$C_{12}H_{23}NO_4$	7.252	0.63976	0.00021877
Level 3	Meta_613	MFCD00005122/Cis-stilbene oxide		$C_{14}H_{12}O$	12.98	2.341	1.6482E-05

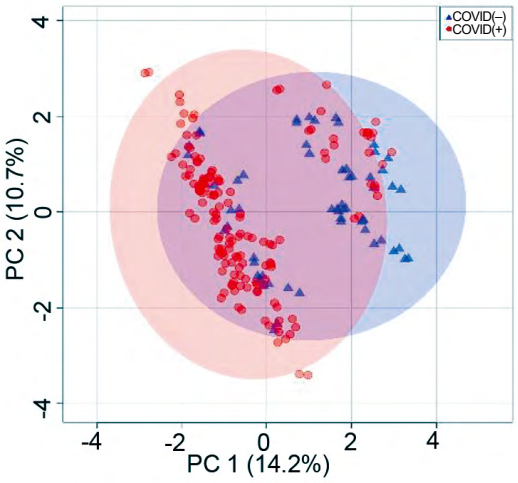

Fig. 5. PCA plot for COVID-19(+) and COVID-19(–) plasma samples.

oxycholic acid, 2-methylbutyrylcarnitine and 1728235/monoacylglyceride were found to be of level-2 MSI (Table 2). All the 6 metabolites were an almost exact match with 2 or more fragment spectral peak matching with HMDB spectral database. Level 3 needs confirmation. Meta_2040 and Meta_2446 were found to be of MSI 4 (***Table S2***). A PCA plot (**Fig. 7**) and heat map (**Fig. 8**) using these 9 metabolites shows the segregation of NSC from SC sample sets. The volcano plot showing 9 significantly altered metabolites in the NSC and SC patient cohort; out of which 4 metabolites are upregulated in the COVID-19(+) cohort and the rest 5 metabolites are down-regulated (**Fig. 9**). The box plots represent annotated metabolites i.e., 7 out of 9 significant DEMs (Fig. 9), and boxplots for unannotated metabolites are represented in *Fig. S1, C*.

Swab metabolome of COVID-19 patient cohorts

The PCA plot exhibited the proper segregation of QC pools from all the swab samples which suggests QC pass for sample run, shown in **Fig. 10**. The correlation matrix between COVID-19(+) and COVID-19(–) samples represented in ***Fig. S2****, A–F*. 30 metabolites were found to be significant DEMs in COVID-19(–) and COVID-19(+) swab samples having a *p*-value less than 0.05 and fold change above 1.5 (**Table 3**). Post blank subtraction 29 significant metabolites were found significant. Out of the 29 metabolites, 7 metabolites were level-2 annotated: 2-isopropyl-N,2,3-trimethylbutanamide, Indane, 1,1'-sulfinyldibenzene, cyromazine, 4,7-dimethylbenzofuran, meglutol, and furfural diethyl acetal (Table 3). Rest of the 22 metabolites were level-4 annotated (***Table S3***). Furthermore, 5 and 1 metabolites were found significantly unique to COVID-19(+) and COVID-19(–) cohort, respectively. Of these, 3 metabolites were level-2 annotated (Table 3), and the rest were level-4 annotated (*Table S3*). The partial least squares-discriminant analysis (PLS-DA) plot was performed based on the 29 significant and non-contaminant classifiers to show the segregation between two cohorts (**Fig. 11**) and heat map preparation to show the segregation of COVID-19(+) from COVID-19(–) cohort (*Fig. S2, H*). The volcano plot shows 29 significantly altered metabolites in the COVID-19(+) and COVID-19(–) patient cohort; out of which 21 metabolites are upregulated in the COVID-19(+) cohort, and the rest 8 metabolites are down-regulated (*Fig. S2, G*). The box plots represent all the level 2 metabolites, i.e., 7 out of 29 significant DEMs are represented in *Fig. S2, G*, and the rest of the unannotated level 4 DEMs were listed in *Table S3*.

NSC and SC swab samples from COVID-19(+) patients' data analysis resulted in 34 features having a *p*-value less than 0.05 and fold change above 1.5 were considered statistically DEMs out of which 20 metabolites were found post blank subtraction. These 20 metabolites were used for PLS-DA plot (**Fig. 12**) and heat map preparation to show the segregation of NSC to SC sample sets (**Fig. 13**). Of the 12, 7 metabolites were level-2 annotated L-threo-sphingosine, phytosphingosine, myristamide, herniarin, 1,1'-sulfinyldibenzene, butoctamide, and meglutol (Table 3). Furthermore, 2 and 1 metabolites were found to be significantly unique to NSC cohort and SC cohort, respectively. Of these 2 metabolites were level-2 annotated (Table 3), and the remaining one was level-4 annotated. The volcano plot shows 20 significantly altered metabolites in the COVID-19(+) and COVID-19(–) patient cohort; of these 13 metabolites are upregulated in the NSC cohort and the rest 7 metabolites are down-regulated (**Fig. 14**).

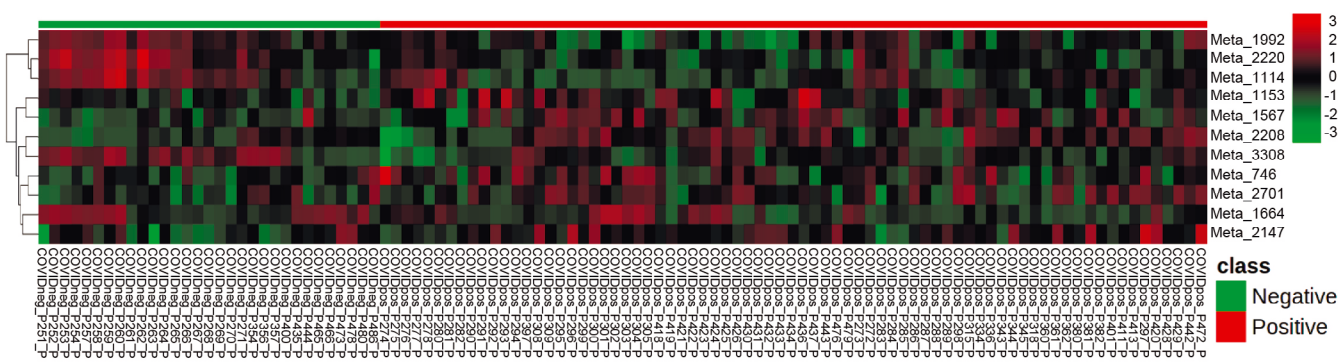

Fig. 6. Heat map of significantly altered metabolites in COVID-19(+) COVID-19(–) patient cohort.

JOURNAL OF MICROBIOLOGY, EPIDEMIOLOGY AND IMMUNOBIOLOGY. 2021; 98(4)
DOI: https://doi.org/10.36233/0372-9311-161
ORIGINAL RESEARCHES

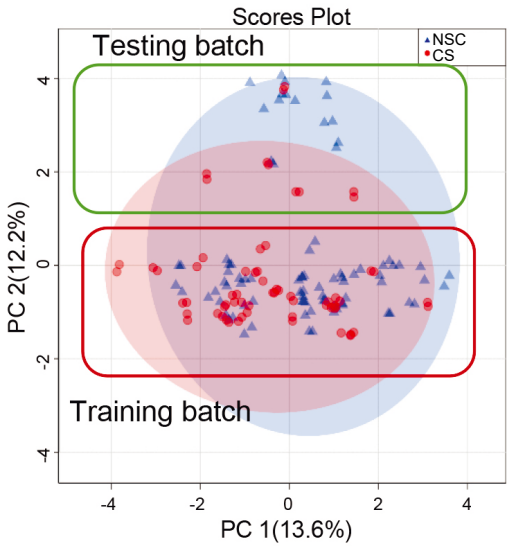

Fig. 7. PCA plot for NSC and SC plasma samples used in the study.

The box plots represent all the level-2 metabolites i.e., 7 out of 20 significant DEMs in Fig. 14, and the rest of the unannotated level-4 DEMs were listed in ***Table S4***.

In case of COVID-19(–) cohort cyromazine, meglutol, 2-isopropyl-N,2,3-trimethylbutanamide, benzocyclopentane were found to be negatively correlated whereas, cyromazine, furfural diethyl acetal, 1,1'-sulfinyldibenzene, 2-isopropyl-N-2,3-triethylbutanamide, benzocyclopentane were found to be positively correlated. On one hand, herniarin, phytosphingosine, butoctamide and DA9185000 (1,1'-sulfinyldibenzene) were negatively correlated in NSC patient cohort. Whereas herniarin, threo-sphingosine, myristamide, 3-hydroxy-3-methylpentanedioic acid (meglutol) and butactamide were found to be positively correlated in NSC sample cohort (**Fig. 15**). On the other hand, herniarin, threo-sphongosine, butoctamide, 3-hydroxy-3-methylpentanedioic acid, DA9185000 (1,1'-sulfinyldibenzene) were found to be negatively

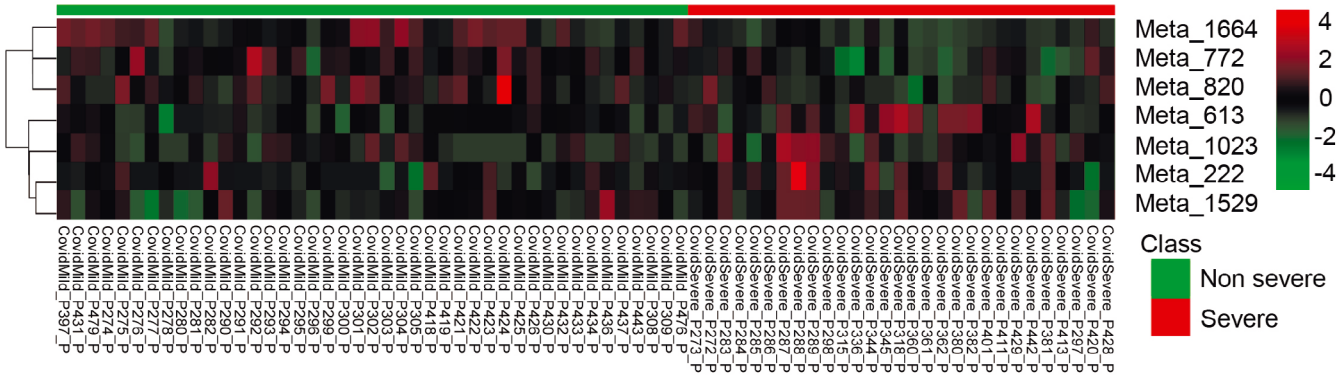

Fig. 8. Heat map of significantly altered metabolites in NSC and SC patient cohort.

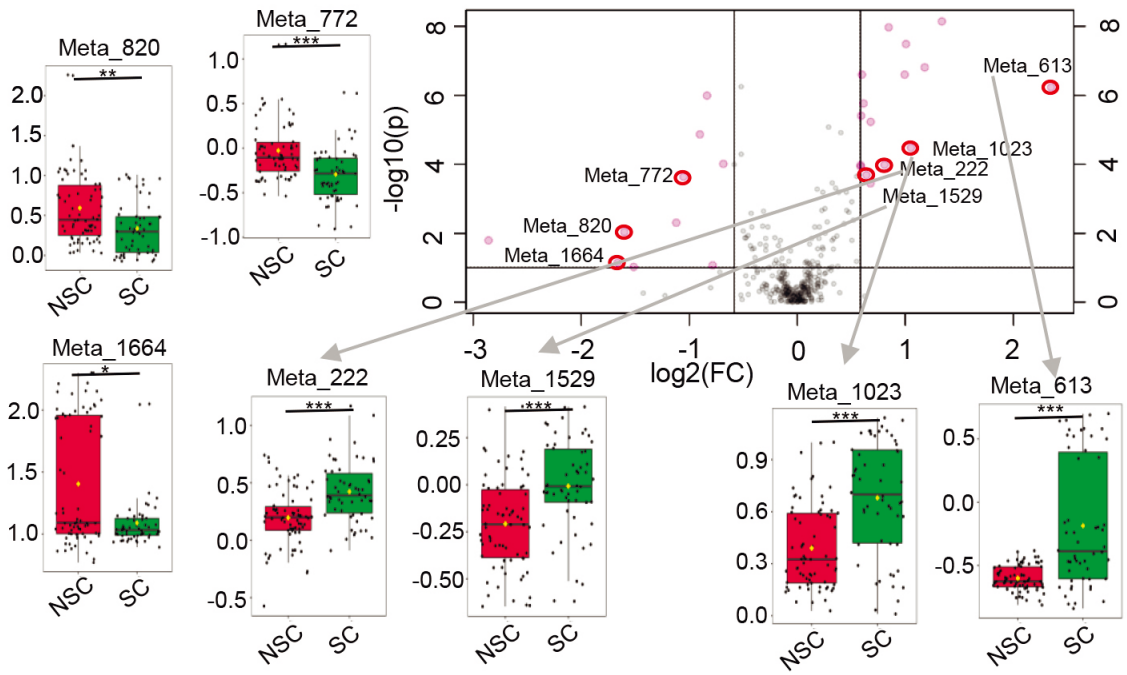

Fig. 9. Volcano plot representing the trend of significant metabolites in NSC patients as compared to SC patients.

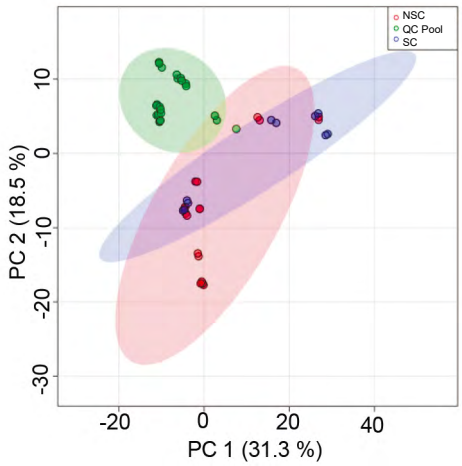

Fig. 10. PCA plot representing proper segregation of QC pools from all the batches for QC of swab sample runs.

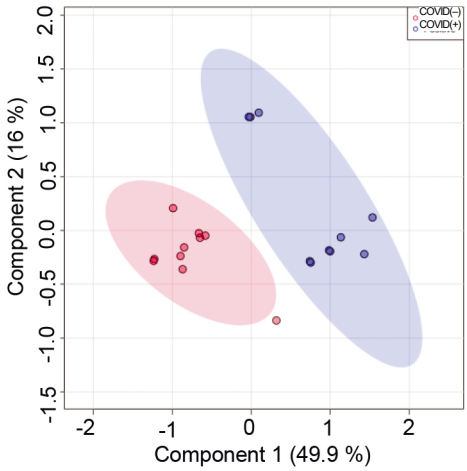

Fig. 11. PLS-DA plot of COVID-19(+) and COVID-19(–) patient cohort.

correlated in SC patient cohort. However, herniarin, butoctamide, myristamide and 3-hydroxy-3-methylpentanedioic acid (meglutol), and phytosphongosine were positively correlated in SC patient cohort (Fig. 15).

Pathway analysis of plasma and swab based metabolome

Pathway analysis was done for all the significant metabolites with HMDB ID using "Metaboanalyst"

Table 3. List of significant metabolites from swab of COVID-19(–), NSC and SC cohorts

List of expressed metabolites in COVID-19(+) patients as compared to COVID-19(–) patients							
Level	MetaCode	Name	Formula	Retention time	Log_2(FC)	Raw *p* value	Type
Level 2	Met_685	1,2,6-Hexanetriol	$C_6H_{14}O_3$	6.888	N/A	N/A	Pos
Level 2	Met_712	2-isopropyl-N,2,3-trimethylbutanamide	$C_{10}H_{21}NO$	11.832	0.58598	0.035932	DEM
Level 2	Met_864	γ-Glu-leu	$C_{11}H_{20}N_2O_5$	7.322	N/A	N/A	Neg
Level 2	Met_984	Indane	C_9H_{10}	14.989	0.69573	0.008432	DEM
Level 2	Met_1820	1,1'-Sulfinyldibenzene	$C_{12}H_{10}OS$	1.313	–0.70988	0.01936	DEM
Level 2	Met_1898	Cyromazine	$C_6H_{10}N_6$	8.787	–0.74273	0.02086	DEM
Level 2	Met_2641	4,7-Dimethylbenzofuran	$C_{10}H_{10}O$	14.988	0.596	0.00392	DEM
Level 2	Met_2709	Meglutol	$C_6H_{10}O_5$	1.277	–0.65851	0.03299	DEM
Level 2	Met_2934	(S)-ATPA	$C_{10}H_{16}N_2O_4$	10.836	N/A	N/A	Pos
Level 2	Met_3339	Furfural diethyl acetal	$C_9H_{14}O_3$	7.779	–0.69864	0.00442	DEM
List of DEMs in NSC patient cohort as compared to SC patients							
Level	MetaCode	Name	Formula	Retention time	Log_2(FC)	FDR adjusted *p* value	Type
Level 2	Met_250	L-Threo-spingosine	$C_{18}H_{37}NO_2$	13.761	–0.78405	0.0135	DEM
Level 2	Met_372	2,3-Naphthalenediol	$C_{10}H_8O_2$	8.817	N/A	N/A	NSC
Level 2	Met_414	Phytosphingosine	$C_{18}H_{39}NO_3$	15.276	–0.6108	0.03107	DEM
Level 2	Met_534	1-Octadecanamine	$C_{18}H_{39}N$	18.086	N/A	N/A	SC
Level 2	Met_719	Myristamide	$C_{14}H_{29}NO$	17.632	1.2395	0.0135	DEM
Level 2	Met_1163	Herniarin	$C_{10}H_8O_3$	10.888	0.63285	0.00518	DEM
Level 2	Met_1960	1,1'-Sulfinyldibenzene	$C_{12}H_{10}OS$	1.317	–0.67829	0.0135	DEM
Level 2	Met_2189	Butoctamide	$C_{16}H_{29}NO_5$	7.383	2.0833	0.04522	DEM
Level 2	Met_2926	Meglutol	$C_6H_{10}O_5$	1.284	–1.0558	4E-05	DEM

Note. Neg — uniquely expressed metabolites in COVID-19(–) patients; Pos — uniquely expressed metabolites in COVID-19(+) patients; NSC — uniquely expressed metabolites in NSC patients; SC — uniquely expressed metabolites in SC patients.

JOURNAL OF MICROBIOLOGY, EPIDEMIOLOGY AND IMMUNOBIOLOGY. 2021; 98(4)
DOI: https://doi.org/10.36233/0372-9311-161
ORIGINAL RESEARCHES

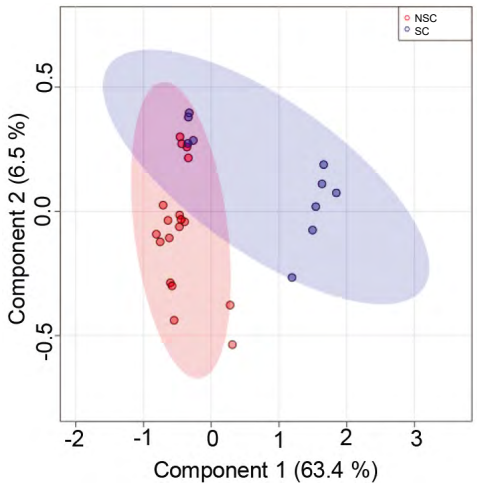

Fig. 12. PLS-DA plot of NSC and SC patient cohort.

and l-α-glycerylphosphorylcholine was found to be enriched in the retinol pathway, and arachidonic acid was mapped to α-linolenic acid and linoleic acid metabolism, arachidonic acid metabolism (*Table S1*). Dioctyltin, bis(4-ethylbenzylidene)sorbitol and arachidonic acid were positively correlated and l-α-glycerylphosphorylcholine, bis(4-ethylbenzylidene)sorbitol and dioctyltin were negatively correlated in the COVID-19(–) patients. However, all the 4 metabolites were found to be positively correlated in the COVID-19(+) patient cohort. Furthermore, in COVID-19(+) patients, correlation was analyzed between NSC and SC patient cohorts.

Creatine and glycochenodeoxycholic acid along with diethylhexyl adipate, 1-monopalmitoylglyverol, acetyltributyl citrate and 10-hydroxmatricaric acid with cis-stilbene oxide were found to be negatively correlated in SC patient cohort. Funtumine, diethylhexyl adipate, DL-propylene glycol dibenzoate and acetyl tributyl citrate were found to be positively correlated in SC cohort.

On the other hand, diethylhexyl adipate, cis-stilbene oxide, DL-propylene glycol dibenzoate, funtumine, and 2-methylbutyroyl carnitine were found to

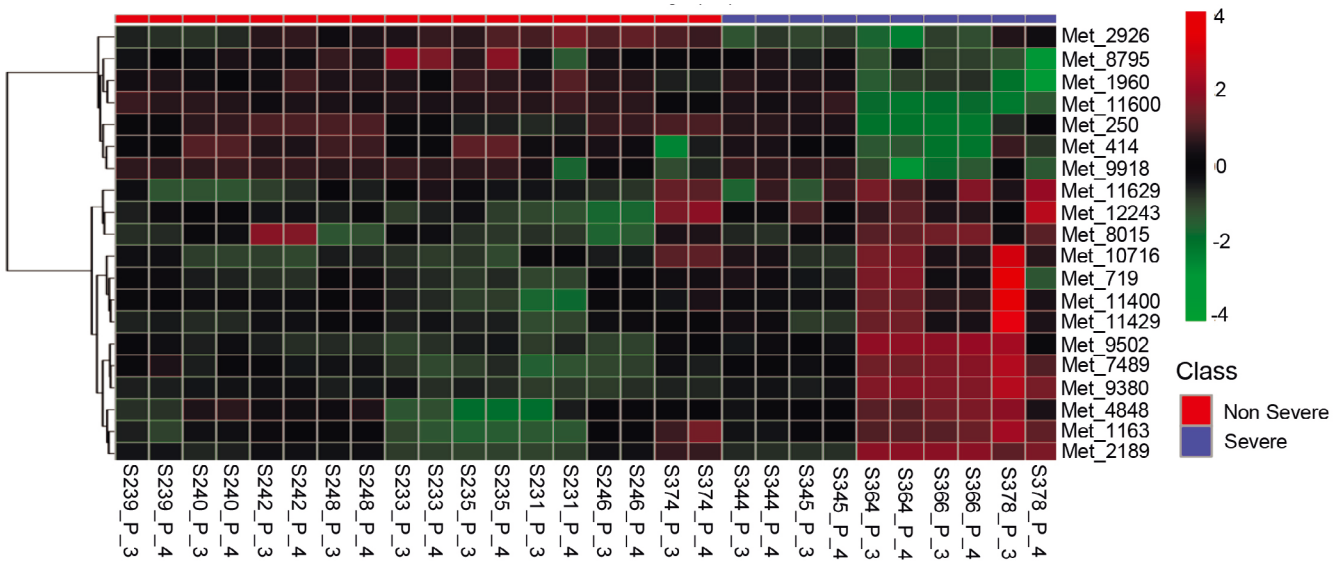

Fig. 13. Heat map of significantly altered metabolites in non-severe and severe COVID-19 patient cohort.

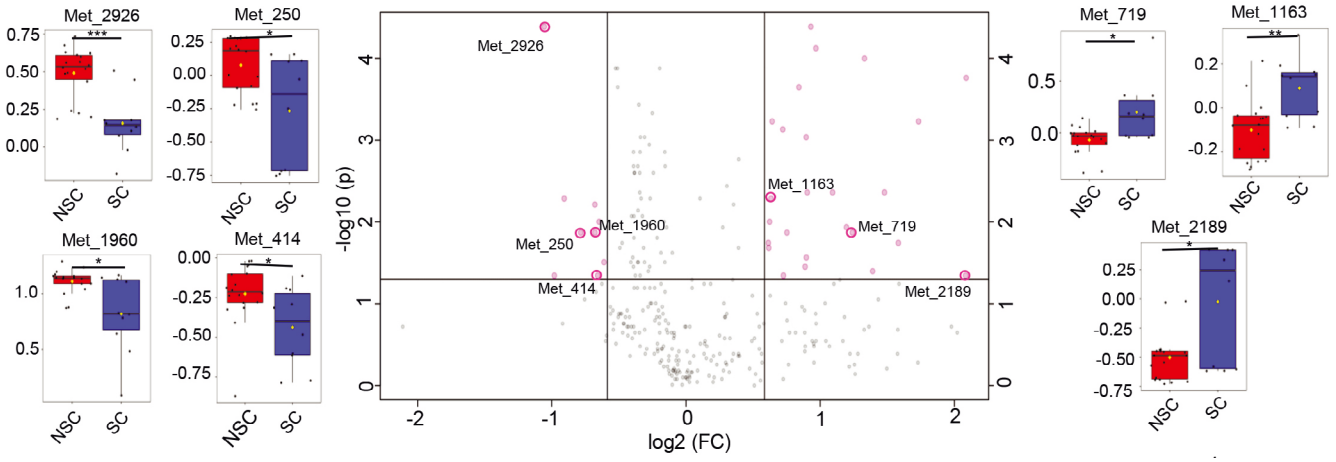

Fig. 14. Volcano plot representing the trends of significantly altered metabolites, level 2 MSI, in NSC and SC patient cohort.

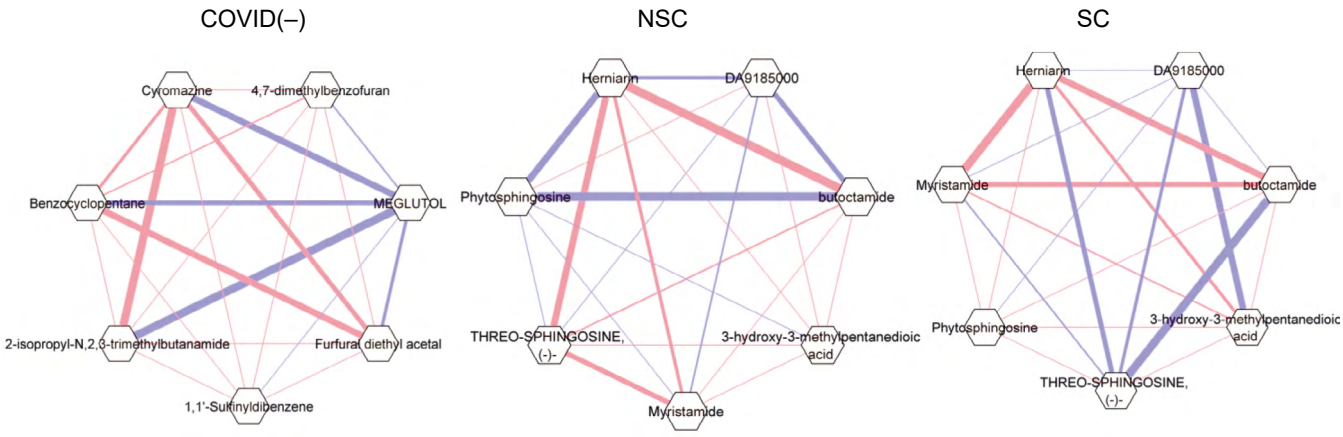

Fig. 15. Correlation among the significantly altered metabolites in the COVID-19(–) samples and COVID-19(+) swab samples (NSC and SC).

be negatively correlated in NSC patient cohort. However, diethylhexyl adipate, funtumine, acetyl tributyl citrate, and DL-propylene glycol dibenzoate were found to be positively correlated same as the SC patient cohort (**Fig. 16**). Propionylcarnitine was found enriched in oxidation of branched chain fatty acids pathway, indole-3-acetic acid was enriched and mapped to tryptophan metabolism pathway, creatine was enriched and mapped to glycine, serine, threonine, arginine, and proline metabolism pathway. Also, glycochenodeoxycholic acid was mapped to bile acid biosynthesis pathway (**Fig. 17** and *Table S2*).

Exposomes analysis

After doing the exposomic analysis by mapping the unannotated metabolites from the raw data with the blood exposome database, 11 exposomes were found to be differentially expressed in COVID-19(+) compared to COVID-19(–) patients (***Table S5***). Out of these 11 exposomes, 4 were found statistically significant with a fold change of greater than 1.5 and *p*-value of less than 0.05. These 4 compounds are: tabun, (2-benzothiazolylthio) acetic acid, contrastigmin, and deoxymethyl-SA. Out of these 4 compounds, 3 compounds (tabun, (2-benzothiazolylthio) acetic acid, and contrastigmin) were upregulated in COVID-19(+) patients as compared to COVID-19(–) patients. Two compounds (contrastigmin and deoxymethyl-SA) were downregulated in SC patients as compared to NSC patient cohort.

Discussion

We observed a drop in the number of annotated and significant metabolites but the metabolites obtained after this set pipeline were consistent with those pub-

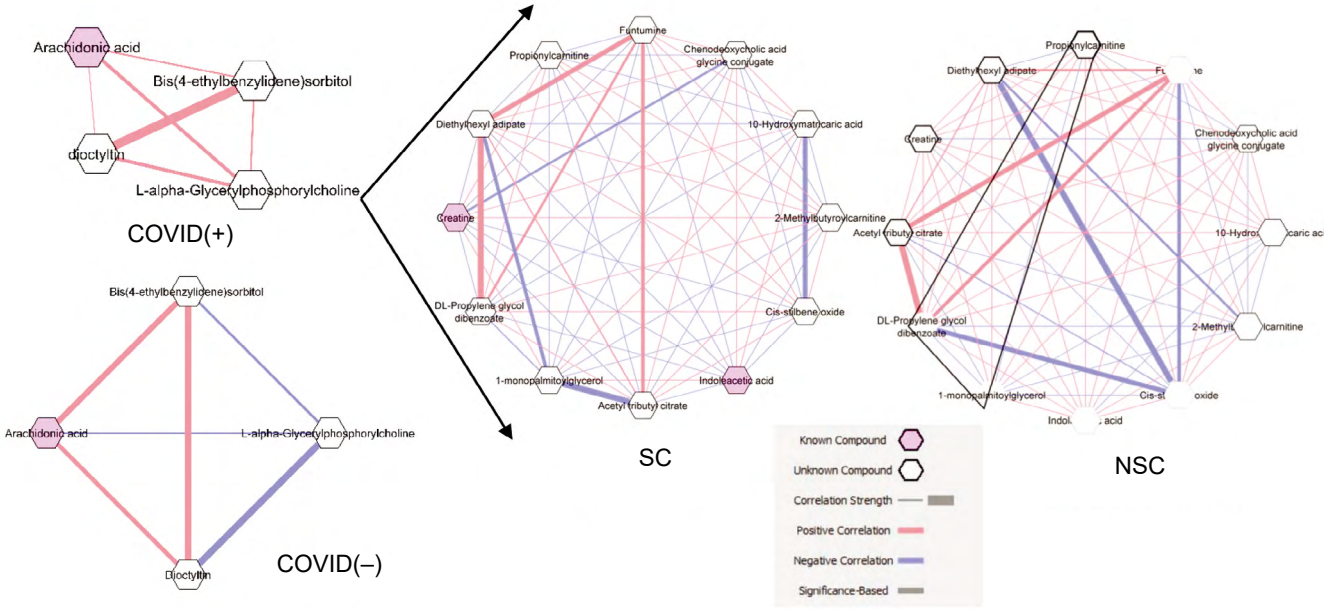

Fig. 16. Correlation among significantly altered metabolites in the COVID-19(–) samples and COVID-19(+) samples (NSC and SC).

JOURNAL OF MICROBIOLOGY, EPIDEMIOLOGY AND IMMUNOBIOLOGY. 2021; 98(4)
DOI: https://doi.org/10.36233/0372-9311-161

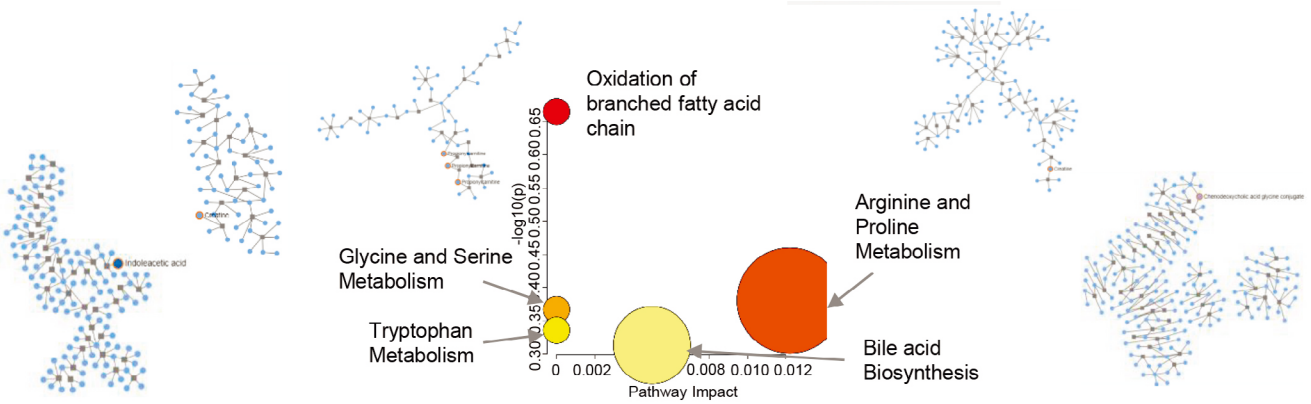

Fig. 17. Pathway analysis of significant metabolites from plasma and swab specimens extracted from NSC and SC patients.

lished works of literature in the context of COVID-19 biology related to the clinical manifestations. Hence, the significant metabolites were explored in the literature for the trend of their alteration in SC and NSC patients (***Tables S6*** and ***S7***).

Plasma metabolome understanding

The upregulation of propionylcarnitine is reported to be significant in the SC patients as compared to the NSC patient cohort, in the alteration of the carnitine pathway (**Fig. 18**) [39–41]. Creatine plays a crucial role in the metabolism of amino acids such as glycine, serine, threonine, arginine, and proline. The upregulation of creatine levels in SC cohort suggests the alteration in amino acid metabolism (Fig. 18) [39, 41–43]. The significantly altered metabolite capturing can be used for the rapid prognosis of the severity of the COVID-19 condition in patients with co-morbidity for efficient healthcare. Another significant metabolite, indole acetic acid, a byproduct product generated due to tryptophan metabolism, is engendered by the modification of tryptophan. However, due to the decrease in tryptophan levels in COVID-19 patients [42], the level of indole acetic acid might be lower than that in COVID-19(–) patients.

Additionally, the conjugate of bile acid-glycine and acyl glycine gives rise to chenodeoxycholic acid glycine conjugate. Most of the bile acids are conjugated with glycine to facilitates fat absorption by solubilization of the fat [44]. The significant downregulation of chenodeoxycholic acid glycine conjugate (Fig. 18) might help in an increase in fat accumulation and imbalance of sodium salt balance [44] in the infected patients prognosing the disease severity in patients with co-morbidities like high cholesterol, hypertension, or heart conditions due to fat accumulation. Additionally, a drug repurposing study unraveled the possibility of chenodeoxycholic acid glycine conjugate/glycochenodeoxycholic acid to be a potential inhibitor of SARS-CoV-2 spike protein RBD which helps in the invasion through ACE2 receptor binding domain [45]. Hence, decrease in chenodeoxycholic acid glycine conjugate/glycochenodeoxycholic acid in the COVID-19(+) patients favors the higher chances of SARS-CoV-2 invasion.

Swab metabolome understanding

In metabolite profiling of swab biospecimens from COVID-19(–), NSC and SC patient, alterations in the phospholipid, fatty acids, sphingomyelins, glycerophospholipids have been reported by B. Yan *et al.* [46]. Alteration in these lipids occurs due to the membrane rearrangement during COVID-19 virus replication in the host. Downregulation of the glycerophospholipids and phospholipids in the case of COVID-19 patients have already been identified in the case of plasma samples [47]. In the case of community-acquired pneumonia (CAP), the level of phospholipids in plasma is low due to the invasive microorganism infection in the host body [48]. Also, the alteration in the oleic acid and arachidonic acid is leading towards the severity cases in COVID-19 patients [46, 49].

In our study, we found that the progression from NSC to SC causing the downregulation of l-threo-sphingosine and phytosphingosine. Sphingosines are the precursors of the sphingolipids present in the cell membrane which helps in the cell permeability and mainly helps in the synthesis of ceramide. L-threo-sphingosine is a stereoisomer of sphingosine which acts as the protein kinase C inhibitor in the mitogen-activated protein kinase (MAPK) pathway [50]. It plays a major role in the induction of apoptosis by inhibiting cell proliferation via inhibition of the MAPK pathway. Phytosphingosine belongs to the sphingolipid family which is found in yeast, plants, and also in mammals. Phytosphingosine possess an extra hydroxyl group at C-4 in comparison to other sphingosine long-chain bases. In the cell, an odd number of fatty acids integrate to form glycerophospholipids obtained from phytosphingosine [51]. These phospholipids are the major component of the cell membrane, which involves various cellular processes such as cell proliferation, cell signaling, cell-cell

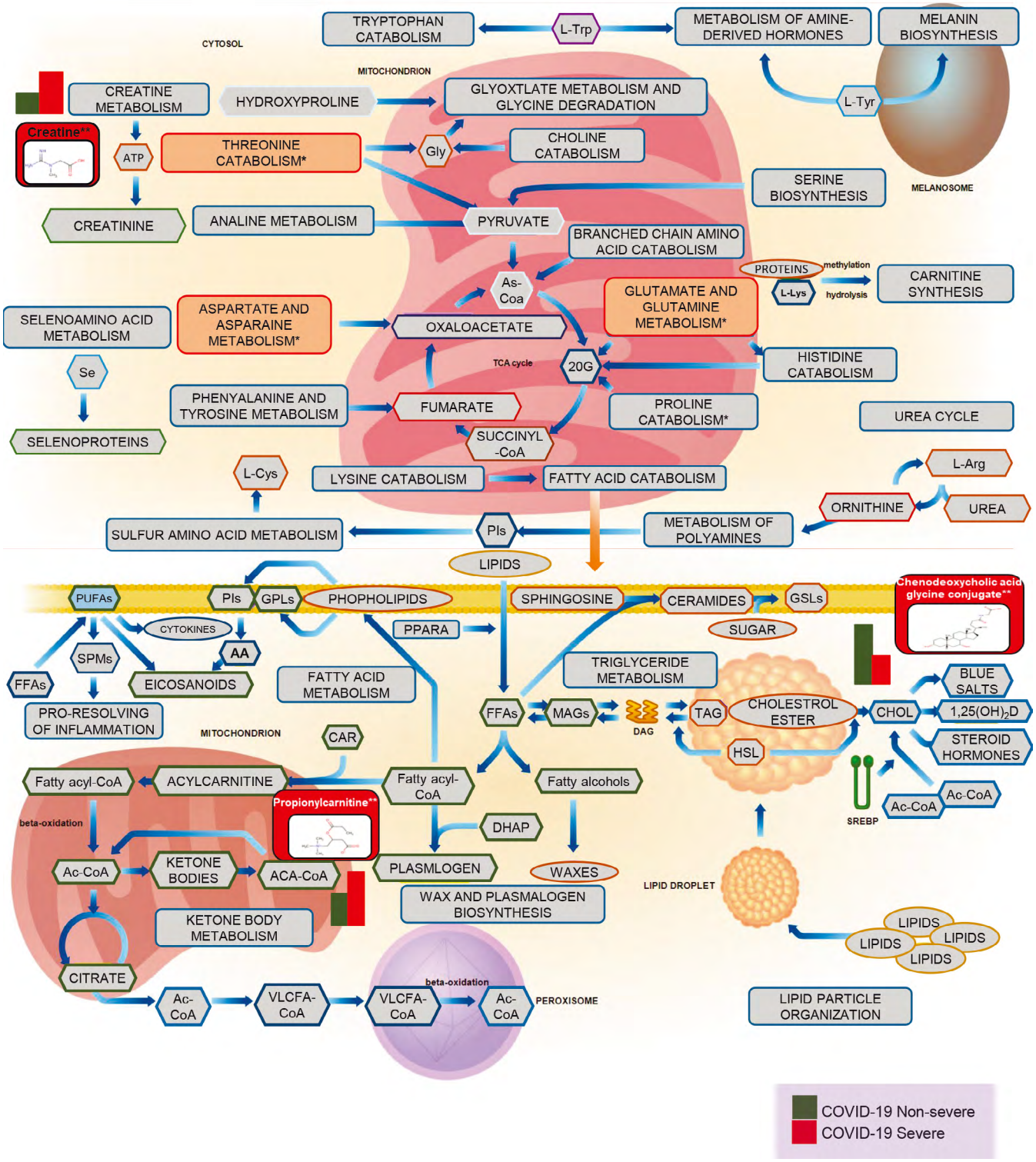

Fig. 18. Pathway analysis of significant metabolites from plasma and swab specimens extracted from NSC and SC patient cohort.

A. Oxidation of branched fatty acid pathway mapping propionylcarnitine. The propionylcartinitine was found to be overexpressed as compared to non-severe patients;
B. Bile acid biosynthesis pathways mapping the chenodeoxycholic acid glycine conjugate and found to be overexpressed in the non-severe patients;
C. Arginine and proline synthesis pathway mapping creatine.
Creatine was found to be overexpressed in the severe patients as compared to non-severe patients.
The mapped metabolites from the study are highlighted in red,
blue highlights are the interacting biomolecules to result in alteration of the effected pathways.

JOURNAL OF MICROBIOLOGY, EPIDEMIOLOGY AND IMMUNOBIOLOGY. 2021; 98(4)
DOI: https://doi.org/10.36233/0372-9311-161

interaction, and cell apoptosis. Like l-threo-sphingosine, phytosphingosine plays a major role in cell apoptosis. Phytosphingosine induces the mitochondria to release caspase-independent cytochrome c which helps apoptosis of T-cell lymphocytes in mammals [52].

It has been shown that upregulation of fatty acids in the body shows a host response against the virus due to activation of a defense mechanism in the host body. These fatty acids are also involved in inflammation which regulates the levels of cytokines in the body. Due to the invasive microorganism host body develops a defense mechanism that induces the release of cytokines, leading to the formation of unsaturated fatty acids in the host body [53]. In our study, we found myristamide to be upregulated in the case of SC patients. Myristamide is an amide form of myristic acid, which is derived from a tetra decanoic acid [54]. On comparing the non-severe with SC cohort, meglutol also known as 3-hydroxy-3-methylpentanedioic acid is downregulated in SC patients. It is a dicarboxylic acid, which is a derivative product of glutaric acid. Meglutol is mainly involved in the transformation of acetate to hydroxymethylglutaryl coenzyme A which lowers the phospholipid level [55].

Role of exposome in COVID-19

Exposomes are the compounds that we get exposed to during our daily life and living habits such as medicinal drugs, food supplements, habits such as smoking, chewing tobacco or consuming alcohol, and any other exposome from the environment that is not found naturally the human system. Exposome-wide association studies have shown a novel approach towards understanding the relationships of several chemical and non-chemical exposures in the progression of human diseases over the course of life and possibly across generations [56, 57]. In case of infectious diseases, the compiled description and evaluation of the exposome components can help in tailoring and evaluation of health disparities and other risk factors (e.g. co-exposure to chemicals, pollution *etc.*) [58]. In this study, we have attempted to identify few exogenous metabolites significant in COVID-19 utilizing a new data analysis method to comprehensively understand COVID-19 pathogenesis in relation to the external environment.

One of the significant blood exposome observed in severe COVID-19 patients is tabun, which is related to cholinesterase inhibitors drugs. The neurotransmitter acetylcholine is hydrolyzed, and thereby inactivated, by cholinesterases [59]. Another exogenous compound (2-benzothiazolylthio) acetic acid has also been observed to be significantly altered in severe patients. It was very interesting to note that benzothiazole derivatives have been reported to be a compound of exogenous origin and used as fungicides, corrosion inhibitors, and vulcanization accelerators in industry [60]. Contrastigmin, also known as pralidoxime methyl sulfate, is a constituent of antidotes: cholinesterase reactivators. These compounds are an important component of therapy in agricultural, industrial, and military poisonings by organophosphates and sulfonates [61]. Also, we observed deoxymethyl-SA, also known as 1-deoxymethylsphinganine, is a compound of endogenous origin and is related to the sphingolipid metabolic pathways [62].

The major focus for conducting this analysis was several unannotated compounds after annotating the data using CD. The probable reason is the existence of several compounds in the samples which are not directly involved in metabolic pathways in the human body, unreported byproducts or compounds of exogenous origin which are not included in HMDB. These compounds can be explored by incorporating databases like blood exposome and other exposomics databases, which will consider the various compounds that a person is exposed to in the environment. In this study, the differential expression of these compounds was studied among various COVID-19 patients to get an insight into potential markers for this disease that may not be directly involved in any biological pathway but exists in the blood due to the dynamic external environment the individual is exposed. However, the major constraints of the study were the small patient dataset and detailed clinical data were not available for all of the patients.

The findings and observations from this study may be used to modulate the altered pathways as therapeutic agents or for diagnostics and prognostic purposes. Metabolites being highly dynamic and major driving molecules of the disease pathways may lead clinicians to early detection of the disease for efficient treatment resulting reduced rate of mortality due to COVID-19.

Future perspective

The significant metabolites reported in this study are the primary and most recurring metabolites as per our datasets and published literature. One of the major unresolved factors is the role of co-morbidities in the COVID-19 severe or vulnerable patient cohort. The pandemic outbreak pattern revealed that the population vulnerable to the virus was the elderly and the comorbid patients. The vulnerable cohort faced the severe form of the disease to the maximum extent [63]. However, a clear map of the pathways involved in the co-morbidity-related severity in the vulnerable patients remains unraveled. Additionally, exposomes become a part of one's metabolome and may modulate the immune system efficiency in the long term. Various reports have favored the role of one's exposome on one's immunity or vulnerability towards a disease [64–66]. Hence, a deeper insight into the exposomes of not only blood but also other biospecimens will provide much more comprehensive understanding of the various exogenous and endogenous factors that contribute towards

disease severity. Information about the factors and pathways leading to severity might provide a better direction for clinicians to treat and control the pandemic. The co-morbidities suspected to synergize the disease prognosis are majorly lifestyle-based and may have the role of exposures one goes through in their daily lives. Hence, prompting the need for co-morbidity-based studies by systematic cohort recruitment, well-defined inclusion, and exclusion criteria. This will enhance the understanding of the disease pathogeneses with respect to age, race, gender, genetic makeup, and co-morbidities involved.

Data and materials availability

All processed data associated with this study are present in the article or in the supplementary materials on the web page of the journal. Raw data will be available on Metabolights MTBLS2291 and MTBLS2349 for plasma and swab raw files, respectively.

REFERENCES

1. Elsevier. Novel Coronavirus Information Center. Available at: https://www.elsevier.com/connect/coronavirus-information-center
2. Clark N.M., Lynch J.P. Influenza: epidemiology, clinical features, therapy, and prevention. *Semin. Respir. Crit. Care Med*. 2011; 32(4): 373–92. https://doi.org/10.1055/s-0031-1283278
3. Wan S., Xiang Y., Fang W., Zheng Y., Li B., Hu Y., et al. Clinical features and treatment of COVID-19 patients in northeast Chongqing. *J. Med. Virol*. 2020; 92(7): 797–806. https://doi.org/10.1002/jmv.25783
4. Iacobucci G. Long Covid: Damage to multiple organs presents in young, low risk patients. *BMJ*. 2020; 371. https://doi.org/10.1136/bmj.m4470
5. Wang D., Hu B., Hu C., Zhu F., Liu X., Zhang J., et al. Clinical characteristics of 138 hospitalized patients with 2019 novel coronavirus-infected pneumonia in Wuhan, China. *JAMA*. 2020; 323(11): 1061–9. https://doi.org/10.1001/jama.2020.1585
6. Zhou F., Yu T., Du R., Fan G., Liu Y., Liu Z., et al. Clinical course and risk factors for mortality of adult inpatients with COVID-19 in Wuhan, China: A retrospective cohort study. *Lancet*. 2020; 395(10229): 1054–62. https://doi.org/10.1016/s0140-6736(20)30566-3
7. Merckx J., Wali R., Schiller I., Caya C., Gore G.C., Chartrand C., et al. Diagnostic accuracy of novel and traditional rapid tests for influenza infection compared with reverse transcriptase polymerase chain reaction. *Ann. Intern. Med*. 2017; 167(6): 394–409. https://doi.org/10.7326/M17-0848
8. Wu L., Qu X. Cancer biomarker detection: recent achievements and challenges. *Chem. Soc. Rev.* 2015; 44(10): 2963–97. https://doi.org/10.1039/C4CS00370E
9. Pegalajar-Jurado A., Fitzgerald B.L., Islam M.N., Belisle J.T., Wormser G.P., Waller K.S., et al. Identification of urine metabolites as biomarkers of early Lyme disease. *Sci. Rep*. 2018; 8(1): 12204. https://doi.org/10.1038/s41598-018-29713-y
10. Weiner J., Maertzdorf J., Sutherland J.S., Duffy F.J., Thompson E., Suliman S., et al. Metabolite changes in blood predict the onset of tuberculosis. *Nat. Commun*. 2018; 9(1): 5208. https://doi.org/10.1038/s41467-018-07635-7
11. Kang D.W., Ilhan Z.E., Isern N.G., Hoyt D.W., Howsmon D.P., Shaffer M., et al. Differences in fecal microbial metabolites and microbiota of children with autism spectrum disorders. *Anaerobe*. 2018; 49: 121–31. https://doi.org/10.1016/j.anaerobe.2017.12.007
12. Nalbantoglu S. Metabolomics: basic principles and strategies. *Mol. Med*. 2019. https://doi.org/10.5772/intechopen.88563
13. Franklin, S., Vondriska T.M. Genomes, proteomes, and the central dogma. *Circ. Cardiovasc. Genet*. 2011; 4(5): 576. https://doi.org/10.1161/CIRCGENETICS.110.957795
14. Nägele T. Linking metabolomics data to underlying metabolic regulation. *Front. Mol. Biosci*. 2014; 1: 22. https://doi.org/10.3389/fmolb.2014.00022
15. Allen U.D., Aoki F.Y., Stiver H.G. The use of antiviral drugs for influenza: recommended guidelines for practitioners. *Can. J. Infect. Dis. Med. Microbiol*. 2006; 17(5): 273–84. https://doi.org/10.1155/2006/165940
16. Colson P., Rolain J.M., Lagier J.C., Brouqui P., Raoult D. Chloroquine and hydroxychloroquine as available weapons to fight COVID-19. *Int. J. Antimicrob. Agents*. 2020; 55(4): 105932. https://doi.org/10.1016/j.ijantimicag.2020.105932
17. Gautret P., Lagier J.C., Parola P., Hoang V.T., Meddeb L., Mailhe M., et al. Hydroxychloroquine and azithromycin as a treatment of COVID-19: Results of an open-label non-randomized clinical trial. *Int. J. Antimicrob. Agents*. 2020; 56(1): 105949. https://doi.org/10.1016/j.ijantimicag.2020.105949
18. Grein J., Ohmagari N., Shin D., Diaz G., Asperges E., Castagna A., et al. Compassionate use of remdesivir for patients with severe Covid-19. *N. Engl. J. Med*. 2020; 382(24): 2327–36. https://doi.org/10.1056/nejmoa2007016
19. Savarino A., Di Trani L., Donatelli I., Cauda R., Cassone A. New Insights into the antiviral effects of chloroquine. *Lancet Infect. Dis*. 2006; 6(2): 67–9. https://doi.org/10.1016/S1473-3099(06)70361-9
20. Vincent M.J., Bergeron E., Benjannet S., Erickson B.R., Rollin P.E., Ksiazek T.G., et al. Chloroquine is a potent inhibitor of SARS coronavirus infection and spread. *Virol. J*. 2005; 2: 69. https://doi.org/10.1186/1743-422X-2-69
21. Touret F., de Lamballerie X. Of chloroquine and COVID-19. *Antiviral Res*. 2020; 177: 104762. https://doi.org/10.1016/j.antiviral.2020.104762
22. Yan Y., Zou Z., Sun Y., Li X., Xu K. F., Wei Y., et al. Anti-malaria drug chloroquine is highly effective in treating avian influenza a H5N1 virus infection in an animal model. *Cell Res*. 2013; 23(2): 300–2. https://doi.org/10.1038/cr.2012.165
23. Gautret P., Lagier J.C., Parola P., Hoang V.T., Meddeb L., Mailhe M., et al. Hydroxychloroquine and azithromycin as a treatment of COVID-19: Results of an open-label non-randomized clinical trial. *Int. J. Antimicrob. Agents*. 2020; 56(1): 105949. https://doi.org/10.1016/j.ijantimicag.2020.105949
24. Jiang C., Wang X., Li X., Inlora J., Wang T., Liu Q., et al. Dynamic human environmental exposome revealed by longitudinal personal monitoring. *Cell*. 2018; 175(1): 277–91.e31. https://doi.org/10.1016/j.cell.2018.08.060
25. Nicholson J.K., Wilson I.D. Understanding "global" systems biology: metabonomics and the continuum of metabolism. *Nat. Rev. Drug Discov.* 2003; 2(8): 668–76. https://doi.org/10.1038/nrd1157
26. Rappaport S.M., Barupal D.K., Wishart D., Vineis P., Scalbert A. The blood exposome and its role in discovering causes of disease. *Environ. Health. Perspect*. 2014; 122(8): 769–74. https://doi.org/10.1289/ehp.1308015
27. Nicholson J.K., Holmes E., Kinross J.M., Darzi A.W., Takats Z., Lindon J.C. Metabolic phenotyping in clinical and surgical environments. *Nature*. 2012; 491(7424): 384–92. https://doi.org/10.1038/nature11708
28. Bray G.A., Redman L.M., de Jonge L., Rood J., Sutton E.F., Smith S.R. Plasma amino acids during 8 weeks of overfeeding: relation to diet body composition and fat cell size in the PROOF study. *Obesity (Silver Spring)*. 2018; 26(2): 324–31. https://doi.org/10.1002/oby.22087
29. Wild C.P. The exposome: from concept to utility. *Int. J. Epidemiol*. 2012; 41(1): 24–32. https://doi.org/10.1093/ije/dyr236

30. Richardson S., Hirsch J.S., Narasimhan M., Crawford J.M., McGinn T., Davidson K.W., et al. Presenting characteristics, comorbidities, and outcomes among 5700 patients hospitalized with COVID-19 in the New York city area. *JAMA*. 2020; 323(20): 2052. https://doi.org/10.1001/jama.2020.6775
31. Su Y., Chen D., Yuan D., Lausted C., Choi J., Dai C.L., et al. Multi-omics resolves a sharp disease-state shift between mild and moderate COVID-19. *Cell*. 2020; 183(6): 1479–95.e20. https://doi.org/10.1016/j.cell.2020.10.037
32. Chen Y.M., Zheng Y., Yu Y., Wang Y., Huang Q., Qian F., et al. Blood molecular markers associated with COVID-19 immunopathology and multi-organ damage. *EMBO J*. 2020; e105896. https://doi.org/10.15252/embj.2020105896
33. Bankar R., Suvarna K., Ghantasala S. Proteomic investigation reveals dominant alterations of neutrophil degranulation and MRNA translation pathways in COVID-19 patients. *iScience*. 2021; 24(3): 102135. https://doi.org/10.1016/j.isci.2021.102135
34. Shen B., Yi X., Sun Y., Bi X., Du J., Zhang C., et al. Proteomic and metabolomic characterization of COVID-19 patient sera. *Cell*. 2020; 182(1): 59–72.e15. https://doi.org/10.1016/j.cell.2020.05.032
35. Suvarna K., Salkar A., Palanivel V., Bankar R., Banerjee N., Gayathri J. et al. A multi-omics longitudinal study reveals alteration of the leukocyte activation pathway in COVID-19 patients. *J. Proteome Res*. 2021. doi: 10.1021/acs.jproteome.1c00215.
36. Züllig T., Zandl-Lang M., Trötzmüller M., Hartler J., Plecko B., Köfeler H.C. A metabolomics workflow for analyzing complex biological samples using a combined method of untargeted and target-list based approaches. *Metabolites*. 2020; 10(9): 1–12. https://doi.org/10.3390/metabo10090342
37. Chong J., Wishart D.S., Xia J. Using MetaboAnalyst 4.0 for comprehensive and integrative metabolomics data analysis. *Curr. Protoc. Bioinformatics*. 2019; 68(1): e86. https://doi.org/10.1002/cpbi.86
38. Chong J., Xia J. MetaboAnalystR: An R package for flexible and reproducible analysis of metabolomics data. *Bioinformatics*. 2018; 34(24): 4313–4. https://doi.org/10.1093/bioinformatics/bty528
39. Maras J.S., Sharma Sh., Bhat A., Rooge Sh., Aggrawal R., Gupta E., Sarin Sh.K. Multi-omics analysis of respiratory specimen characterizes baseline molecular determinants associated with SARS-CoV-2 outcome. *iScience*. 2021; 24(8): 102823. https://doi.org/10.1016/j.isci.2021.102823.
40. Mohammed A., Alghetaa F.K.H., Miranda K., Wilson K., Singh P.N., Cai G., et al. Δ9-tetrahydrocannabinol prevents mortality from acute respiratory distress syndrome through the induction of apoptosis in immune cells, leading to cytokine storm suppression. *Int. J. Mol. Sci*. 2020; 21(17): 6244. https://doi.org/10.3390/ijms21176244
41. Roberts I., Muelas M.W., Taylor J.M., Davison A.S., Xu Y., Grixti J.M., et al. Untargeted metabolomics of COVID-19 patient serum reveals potential prognostic markers of both severity and outcome. *medRxiv*. 2020; 2020.12.09.20246389. https://doi.org/10.1101/2020.12.09.20246389
42. Thomas T., Stefanoni D., Reisz J.A., Nemkov T., Bertolone L., Francis R.O., et al. COVID-19 infection alters kynurenine and fatty acid metabolism, correlating with IL-6 levels and renal status. *JCI Insight.* 2020; 5(14): e140327. https://doi.org/10.1172/jci.insight.140327
43. Fraser D.D., Slessarev M., Martin C.M., Daley M., Patel M.A., Miller M.R., et al. Metabolomics profiling of critically ill coronavirus disease 2019 patients: identification of diagnostic and prognostic biomarkers. *Crit. Care Explor*. 2020; 2(10): e0272. https://doi.org/10.1097/CCE.0000000000000272
44. Goto T., Myint K.T., Sato K., Wada O., Kakiyama G., Iida T., et al. LC/ESI-Tandem mass spectrometric determination of bile acid 3-sulfates in human urine 3beta-sulfooxy-12alpha-hydroxy-5beta-cholanoic acid is an abundant nonamidated sulfate. *J. Chromatogr. B Analyt. Technol. Biomed. Life. Sci*. 2007; 846(1–2): 69–77. https://doi.org/10.1016/j.jchromb.2006.08.013
45. Carino A., Moraca F., Fiorillo B., Marchianò S., Sepe V., Biagioli M., et al. Hijacking SARS-Cov-2/ACE2 receptor interaction by natural and semi-synthetic steroidal agents acting on functional pockets on receptor binding region. *Pharmacol. Toxicol*. Preprint. 2020. https://doi.org/10.1101/2020.06.10.144964
46. Yan B., Chu H., Yang D., Sze K.H., Lai P.M., Yuan S., et al. Characterization of the lipidomic profile of human coronavirus-infected cells: implications for lipid metabolism remodeling upon coronavirus replication. *Viruses*. 2019; 11(1). https://doi.org/10.3390/v11010073
47. Wu D., Shu T., Yang X., Song J.X., Zhang M., Yao C., et al. Plasma metabolomic and lipidomic alterations associated with COVID-19. *Natl. Sci. Rev.* 2020; 7(7): 1157–68. https://doi.org/10.1093/nsr/nwaa086
48. Arshad H., Alfonso J.C.L., Franke R., Michaelis K., Araujo L., Habib A., et al. Decreased plasma phospholipid concentrations and increased acid sphingomyelinase activity are accurate biomarkers for community-acquired pneumonia. *J. Transl. Med*. 2019; 17(1): 1–18. https://doi.org/10.1186/s12967-019-2112-z
49. Barberis E., Timo S., Amede E., Vanella V.V., Puricelli C., Cappellano G., et al. Large-scale plasma analysis revealed new mechanisms and molecules associated with the host response to Sars-Cov-2. *Int. J. Mol. Sci*. 2020; 21(22): 8623. https://doi.org/10.3390/ijms21228623
50. Bode C., Berlin M., Röstel F., Teichmann B., Gräler M.H. Evaluating sphingosine and its analogues as potential alternatives for aggressive lymphoma treatment. *Cell. Physiol. Biochem*. 2014; 34(5): 1686–700. https://doi.org/10.1159/000366370
51. Merrill A.H., Sandhoff K. Chapter 14 sphingolipids: metabolism and cell signaling. *New Compr. Biochem*. 2002; 36: 373–407. https://doi.org/10.1016/s0167-7306(02)36016-2
52. Bielawski J., Pierce J.S., Snider J., Rembiesa B., Szulc Z.M., Bielawska A. Sphingolipid analysis by high performance liquid chromatography-tandem mass spectrometry (HPLC-MS/MS). In: Chalfant C., Poeta M.D., eds. *Sphingolipids as Signaling and Regulatory Molecules. Advances in Experimental Medicine and Biology.* New York, NY: Springer; 2010; 46–59. https://doi.org/10.1007/978-1-4419-6741-1_3
53. Das U.N. Arachidonic acid and other unsaturated fatty acids and some of their metabolites function as endogenous antimicrobial molecules: a review. *J. Adv. Res*. 2018; 11: 57–66. https://doi.org/10.1016/j.jare.2018.01.001
54. Castillo-Peinado L.S., López-Bascón M.A., Mena-Bravo A., Luque de Castro M.D., Priego-Capote F. Determination of primary fatty acid amides in different biological fluids by LC–MS/MS in MRM mode with synthetic deuterated standards: influence of biofluid matrix on sample preparation. *Talanta*. 2019; 193: 29–36. https://doi.org/10.1016/j.talanta.2018.09.088
55. Jones D.E., Perez L., Ryan R.O. 3-Methylglutaric acid in energy metabolism. *Clin. Chim. Acta*. 2020; 502: 233–9. https://doi.org/10.1016/j.cca.2019.11.006
56. Misra B.B. Metabolomics tools to study links between pollution and human health: an exposomics perspective. *Curr. Pollution. Rep*. 2019; 5(3): 93–111. https://doi.org/10.1007/s40726-019-00109-4
57. Juarez P.D., Matthews-Juarez P. Applying an exposome-wide (ExWAS) approach to cancer research. *Front. Oncol*. 2018; 8: 313. https://doi.org/10.3389/fonc.2018.00313
58. Andrianou X.D., Pronk A., Galea K.S., Stierum R., Loh M., Riccardo F., et al. Exposome-based public health interventions for infectious diseases in urban settings. *Environ. Int.* 2021; 146: 106246. https://doi.org/10.1016/j.envint.2020.106246
59. Adeyinka A., Kondamudi N.P. Cholinergic crisis. In: *StatPearls.* Treasure Island (FL): StatPearls Publishing; 2020.

60. Kloepfer A., Gnirss R., Jekel M., Reemtsma T. Occurrence of benzothiazoles in municipal wastewater and their fate in biological treatment. *Water Sci. Technol*. 2004; 50(5): 203–8.
61. Eddleston M., Buckley N.A. A strategy for changing plasma pralidoxime kinetics and, perhaps, effect in organophosphorus insecticide poisoning. *Crit. Care. Med.* 2011; 39(4): 908–9. https://doi.org/10.1097/CCM.0b013e31820a839b
62. Merrill A.H. Sphingolipid and glycosphingolipid metabolic pathways in the era of sphingolipidomics. *Chem. Rev*. 2011; 111(10): 6387–422. https://doi.org/10.1021/cr2002917
63. Mauvais-Jarvis F. Aging, male sex, obesity, and metabolic inflammation create the perfect storm for COVID-19. *Diabetes*. 2020; 69(9): 1857. https://doi.org/10.2337/dbi19-0023
64. Adams K., Weber K.S., Johnson S.M. Exposome and immunity training: how pathogen exposure order influences innate immune cell lineage commitment and function. *Int. J. Mol. Sci.* 2020; 21(22): 8462. https://doi.org/10.3390/ijms21228462
65. Maguire G. Better preventing and mitigating the effects of COVID-19. *Future Sci. OA*. 2020; 6(6): FSO586. https://doi.org/10.2144/fsoa-2020-0051
66. Land W.G. Role of damage-associated molecular patterns in light of modern environmental research: a tautological approach. *Int. J. Environ. Res*. 2020; 1–22. https://doi.org/10.1007/s41742-020-00276-z

Information about the authors

Shalini Aggarwal — Ph.D., Department of biosciences and bioengineering, Indian Institute of Technology, Mumbai, India, https://orcid.org/0000-0002-5951-2102

Shashwati Parihari — Ph.D., Department of biosciences and bioengineering, Indian Institute of Technology, Mumbai, India, https://orcid.org/0000-0002-3989-019X

Arghya Banerjee — Ph.D., Department of biosciences and bioengineering, Indian Institute of Technology, Mumbai, India, https://orcid.org/0000-0002-0043-5827

Jyotirmoy Roy — student (B. Tech.), Department of chemical engineering, Indian Institute of Technology, Mumbai, India, https://orcid.org/0000-0002-8124-3121

Nirjhar Banerjee — Ph.D., Department of biosciences and bioengineering, Indian Institute of Technology, Mumbai, India, https://orcid.org/0000-0003-3404-9390

Renuka Bankar — postgraduate student (M. Sci.), junior researcher, Indian Institute of Technology Bombay, Mumbai, India, https://orcid.org/0000-0001-8530-5062

Saravanan Kumar — Ph.D. (Life Sci.), team leader — Proteomics, Proteomics Lab, Thermo Fisher Scientific India, Whitefield, Bangalore, India. https://orcid.org/0000-0001-6352-3595

Manisha Choudhury — Ph.D., post-doctoral researcher, Department of biosciences and bioengineering, Indian Institute of Technology Bombay, Mumbai, India, https://orcid.org/0000-0002-6108-9040

Rhythm Shah — student (B. Tech.), Department of metallurgical engineering and materials science, Indian Institute of Technology Bombay, Mumbai, India, https://orcid.org/0000-0002-5963-9816

Kharanshu Bhojak — Student (B. Tech.), Department of metallurgical engineering and materials science, Indian Institute of Technology Bombay, Mumbai, India, https://orcid.org/0000-0001-8917-2965

Viswanthram Palanivel — postgraduate student (MSc. biomedical science), junior researcher, Department of biosciences and bioengineering, Indian Institute of Technology Bombay, Mumbai, India, https://orcid.org/0000-0002-4649-5913

Akanksha Salkar — postgraduate student (MSc. biological sciences), junior researcher, Department of biosciences and bioengineering, Indian Institute of Technology Bombay, Mumbai, India, https://orcid.org/0000-0001-9941-0947

Sachee Agrawal — Assistant Professor, Microbiology, Kasturba Hospital for Infectious Diseases, Chinchpokli, Mumbai, India, SCOPUS ID 56344028500

Om Shrivastav — M.D., Infectious diseases, Kasturba Hospital for Infectious Diseases, Chinchpokli, Mumbai, India, SCOPUS ID 57200535430

Jayanthi Shastri — Professor, Head of Department of microbiology, Kasturba Hospital for Infectious Diseases, Chinchpokli, Mumbai, India, https://orcid.org/0000-0001-7360-564X

Sanjeeva Srivastava✉ — Professor, Department of biosciences and bioengineering, Indian Institute of Technology Bombay, Mumbai, India, sanjeeva@iitb.ac.in, https://orcid.org/0000-0001-5159-6834

Author contribution. SS, SA, and SP contributed to conceiving the idea, and outline. SA, SP, MC, JR, NB, RS wrote the manuscript. SK, SA, SP, NB, and AB were involved in the optimization of the parameters starting from sample preparation to data analysis pipeline for COVID-19 samples. SA and SP performed the analysis and did literature based analysis. SA performed the pathway and correlation analysis. RB, MC, VP and AS collected and prepared the samples. JR and MC performed exposome analysis. SA, SP, RS and KB prepared the figures. Authors SA, SP, AB, JR; NB and RB; RS and KB are contributed equally. All authors made a substantial contribution to the conception of the work, acquisition, analysis, interpretation of data for the work, drafting and revising the work, final approval of the version to be published.

The article was submitted 07.05.2021;
accepted for publication 10.08.2021;
published 30.08.2021